Cost Comparisons for Emerging Carbon Dioxide Removal Technologies

Philip Holler*
MISES, University of Mannheim
philip.holler@uni-mannheim.de

Stefan Reichelstein
MISES, University of Mannheim
Graduate School of Business, Stanford University
ZEW – Leibniz Centre for European Economic Research
reichelstein@uni-mannheim.de

August 2026

*We acknowledge valuable research assistance from Thimo Merke, Florian Othmer, Johannes Minkel, Maurice Beichert and Victoria Groothold. We thank Amadeus Bach and Gunther Glenk for constructive feedback. This study is part of the Greenhouse Gas Removal (GHG-R) Flagship Destination under the Stanford Sustainability Accelerator.

Abstract

This paper develops a techno-economic framework for comparing alternative carbon dioxide removal (CDR) technologies. The key financial cost metric emerging from our framework is the Levelized Cost of CDR (LCCDR). It represents the minimal off-take price per net ton of CO_2 durably removed that an investor would need to receive in order to break even on a given project. Our analysis accounts for leakage (offsetting process emissions) and co-product revenues, including applicable tax subsidies. The four technologies examined here, Biomass Carbon Removal and Storage (BiCRS), Bioenergy with Carbon Capture and Storage (BECCS), Enhanced Rock Weathering (ERW), and Direct Air Capture (DAC), all have the potential to remove CO_2 at gigaton scale. In the context of the current U.S. market and regulatory environment, we identify a remarkably wide interval of LCCDR values ranging from \$29 to \$1,076 per ton of CO_2. We relate our cost findings to prices reported under existing offtake agreements and discuss the potential as well as the remaining uncertainties for each of these four carbon removal technologies.

Keywords: Carbon Dioxide Removal, Levelized Costs, Techno-Economics, System Boundaries, Carbon Accounting, Negative Emissions

JEL Codes: G31, H23, Q52, Q54, Q58

1 Introduction

Global emissions remain above 50 gigatons of carbon dioxide equivalents (CO_2e) per year, far from the net-zero targets adopted by most large economies. Even ambitious abatement efforts, however, are unlikely to eliminate all emissions. Therefore, emission reductions must be combined with large-scale removal of CO_2 from the atmosphere[1]. Carbon dioxide removal (CDR) technologies capture CO_2 from non-fossil sources and store it durably[2]. They have emerged as a critical complement to abatement in global decarbonization pathways[3–5] and can address residual emissions from hard-to-abate sectors, such as long-distance air travel[6;7].

The scale implied by these pathways is far above near-term deployment. Model estimates place annual removals needed in 2050 between 5,000 and 15,000 Mt CO_2[1] [7–10]. While conventional, land-based methods provide almost 2,000 Mt CO_2 of carbon uptake per year, durable pathways contribute only a small fraction[11]. Novel CDR activity stands at around 2 Mt CO_2 per year, and the project pipeline is expected to reach 8.4 Mt CO_2 per year by 2030[12].

Policy is moving to address this gap. In the United States (U.S.), the Carbon Negative Shot targets removals below $100 per ton by 2032[13], while the Inflation Reduction Act's 45Q tax credit pays up to $180 per ton for DAC and $85 for other geologically stored carbon[14]. In the European Union (EU), the Commission has recently proposed to integrate permanent removals into the EU cap and trade system[15;16]. As durable CDR moves toward public procurement and proposed compliance-market integration, governments must decide what constitutes a *net* removal, which system boundaries to consider, and how to design policy support to incentivize atmospheric removal.

It is yet unclear which technologies can deliver cost- and emission-effective removal, given the large techno-economic uncertainty across and within pathways[17;18]. We focus on four technologies with the potential for gigaton-scale CO_2 removal: Biomass Carbon Removal and Storage (BiCRS), Bioenergy with Carbon Capture and Storage (BECCS), Direct Air Capture (DAC), and Enhanced Rock Weathering (ERW). These technologies have so far dominated the voluntary carbon removal market[19].

Figure 1 reports transaction volumes recorded from 2019 to 2025. Contracted volume reached ∼31 $MtCO_2$ in 2025, but only ∼2.3 $MtCO_2$ had been delivered. BECCS dominates the aggregate transactions, BiCRS the delivered volume. The total sold-to-delivered ratio is

[1]Throughout, we report CO_2 quantities as tCO_2. A ton denotes a metric ton (1,000 kg) and Mt denotes a million metric tons.

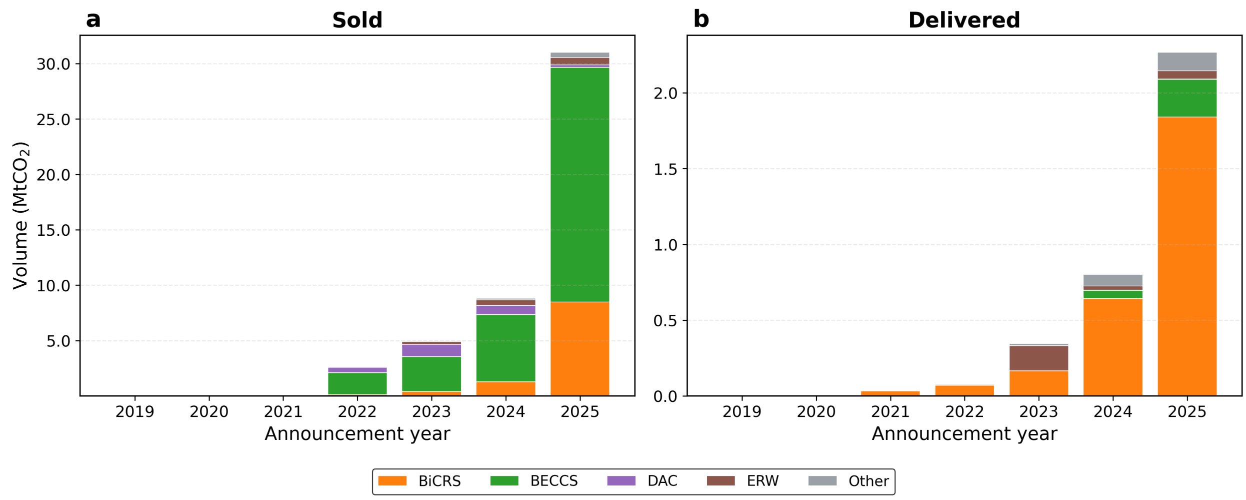

Figure 1. CDR transactions by pathway. Stacked annual volume of voluntary-market CDR transactions by technology from 2019 to 2025[19]. (**a**) aggregates all transactions and represents total volume. (**b**) covers only delivered tons.

about 14:1 and widens to ∼84:1 for BECCS and ∼360:1 for DAC. These gaps mean that most transactions are commitments to future delivery from projects that are not yet operating. Price information is also limited: prices are disclosed for ∼30% of transactions and ∼13% of contracted tonnage, with the disclosed sample skewed toward small biochar and bio-oil orders[19]. Buyers in this young market must therefore evaluate highly heterogeneous forward offers without observable project costs or comparable accounting boundaries.

A disclosed price alone does not identify the cost of removing a net ton. That cost depends on the accounting boundary, feedstock and energy emissions, and the treatment of co-products[20;21]. We therefore introduce three measures. LCCDR is the minimal off-take price per net ton that allows an investor to break even. It includes life-cycle cost components, subtracts co-product sales and policy support and adjusts for attributable emissions. Attributable emissions are summarized in the *leakage factor* α. The second measure, LCCDR$^-$, retains project co-product revenues but ignores attributable emissions, thereby providing a lower bound cost estimate. The third measure, LCCDR$^+$ includes attributable emissions but excludes any co-product revenues, showing the full cost of delivering a net ton. The differences between the three measures identify whether an apparent cost advantage comes from the current process cost, the accounting boundary, or an offsetting revenue stream.

Applying the framework to eighteen current project configurations calibrated to a U.S. setting, we estimate investor break-even prices of \$29–\$1,076 per net ton and leakage factors of 1–41%. Dunite ERW has the lowest modeled range, \$29–\$70 per ton, but this technical frontier depends on the modeled weathering rate, suitable application sites, and site-specific measurement, reporting, and verification (MRV) requirements. The biomass configurations range from \$89 to \$163. Basalt ERW spans \$125–\$340 per ton, overlapping both the biomass and DAC ranges. DAC exhibits the highest current costs despite receiving the largest policy support, at \$245–\$1,076 per ton. These cost ranges are sensitive to the inclusion of attributable emissions and co-product revenues. In particular, 45Q determines which biomass pathway is cheapest. Because 45Q is paid per gross ton captured rather than per net ton removed, its effective value per net ton rises with the leakage factor α. The reduction in investor break-even price therefore ranges from \$82 to \$341 per net ton. Observed BECCS and DAC prices largely overlap the modeled ranges. BiCRS and ERW prices lie above them. This gap indicates that disclosed transaction prices also reflect scarcity, delivery risk, MRV charges, and other unobserved attributes.

Our paper adds to the growing literature estimating the future cost and potential of CDR technologies, such as DAC[17;22–37], BiCRS[38–40], BECCS[41–48] and ERW[38;49–57]. A recent stream of literature suggests that diversified CDR usage can reduce land, energy, and sustainability trade-offs relative to strong reliance on any single removal pathway[58–61]. With operational CDR capacity still far below projected mid-century needs, a transparent cost and system boundary framework is needed for assessing gigaton-scale deployment.

This paper makes two related contributions. First, we develop a common LCCDR framework that separates the effects of attributable emissions, co-product sales, and policy support on the price required for a removal project to break even. Existing comparative work either stops at engineering cost[62;63] or examines sustainability and portfolio trade-offs at the system level[58;59]. It therefore does not isolate how these three factors interact and change project-level costs. Second, we calibrate the framework for eighteen current project configurations. Our analysis compiles engineering studies, government energy and emissions data, registry methodologies, policy rules, and disclosed market transactions. We then harmonize them within a common accounting boundary, responding to the absence of a standardized project-level method for determining net removal[64]. Together, the framework and calibrated configurations provide a common net-ton basis for comparing otherwise dissimilar technologies and project configurations. Our calculations show how accounting boundaries and policy support impact the economics of durable carbon removal.

2 Economic Model

This section develops a generic concept and formal definition for the levelized cost of carbon dioxide removal (LCCDR). In direct analogy to the levelized cost of electricity (LCOE) or the levelized cost of hydrogen (LCOH)[65–67], the LCCDR is conceptualized as the critical price per ton of CO_2 durably removed from the atmosphere that an investor would need in order to break even on a new carbon capture and sequestration facility. The break-even criterion is stated in terms of the applicable life-cycle cash flows, including capital costs, operating expenditures, transport and storage, offsetting emissions, corporate income taxes, and co-product revenues. The LCCDR metric is shown to be highly sensitive to the applicable system boundaries in terms of offsetting emissions and co-product revenues.

To illustrate our LCCDR model framework, suppose an investor considers a new facility that produces bioenergy with carbon capture and storage (BECCS). BECCS facilities are operating at commercial scale today, attracting demand in the voluntary carbon markets from parties that seek to buy carbon removal credits[19]. A representative BECCS plant receives biomass feedstock at the gate (e.g. forestry & agricultural residues, dedicated energy crops), combusts it for heat and power, and routes the flue gas through a post-combustion solvent loop (typically amine-based) that captures CO_2. The captured stream is then compressed and transported via pipeline, ship or truck, before it is injected into a geological reservoir for durable sequestration. Figure 2 illustrates the relevant monetary and carbon emission flows in connection with a BECCS facility. In section 3 below, we discuss the criterion for "durability" in connection with different sequestration technologies.

Beyond BECCS, the following base model is equally applicable to DAC and BiCRS removal processes. In contrast, our base model needs to be modified for ERW processes as the facility in question will only crush rocks that will then be spread out on land in order to sequester CO_2 in subsequent years. We assume that the capture, transportation and sequestration steps are fully synchronized so that it suffices to keep track of tons of CO_2 sequestered in hour t of year i. We denote this quantity by the variable q_{it}, where $1 \leq t \leq m$, with $m \equiv 8,760$, and $1 \leq i \leq T$, with T denoting the useful life of the capture and sequestration facility. The practical capacity size, k, of the plant refers to the maximal value of tons of CO_2 that can be sequestered in any given hour. It can be considered the achievable capacity and accounts for scheduled maintenance and anticipated downtime. Thus $q_{it} \leq k$. In addition, the capacity for sequestration may be volume constrained in terms of the tons

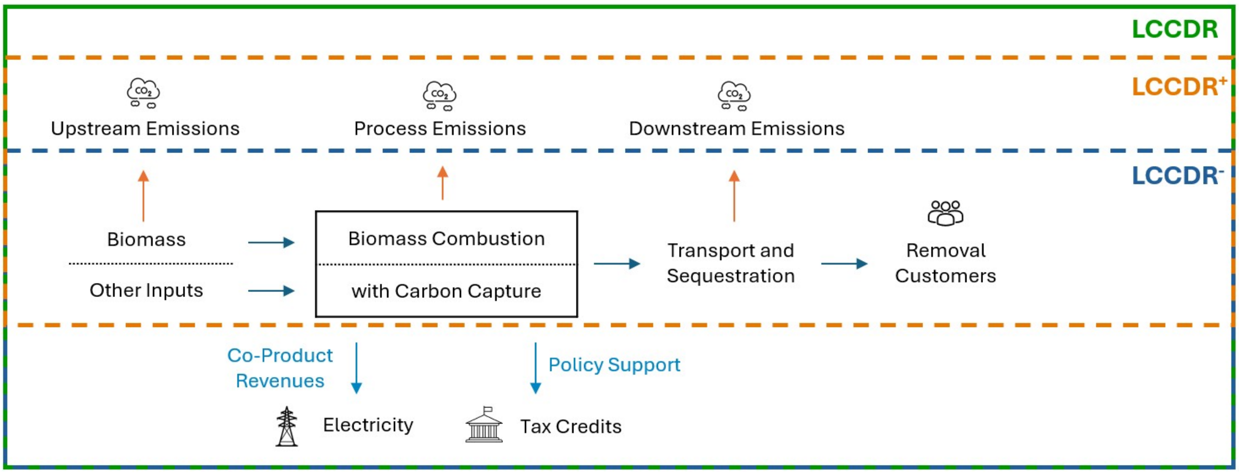

Figure 2. Bioenergy with Carbon Capture and Storage. This figure illustrates the techno-economic setting for a generic BECCS facility. Our base LCCDR calculation presumes system boundaries that account for all emission and revenue sources inside the green box.

of CO_2 that can be maximally sequestered at the particular site.

Companies seeking to acquire carbon credits will frequently only base their calculations and off-take contracts on the *net tons* of CO_2 sequestered. Thus, if the CDR process involves direct emissions, such as those incurred in connection with transportation or operational activities, these emissions need to be netted against q_{it}. Our model framework draws system boundaries that include Scope 1 and Scope 2 emissions. Our base model also accounts for offsets corresponding to emissions embodied in electricity purchased from the grid for either the capture or the sequestration process. We represent these offsetting emissions by the *leakage factor* α, with $0 \leq \alpha \leq 1$, so that the net tons of CO_2 sequestered in any given hour are given by $(1 - \alpha) \cdot q_{it}$.

The representative CDR facility is assumed to be sized so as to take advantage of any applicable economies of scale. The extant literature suggests that an efficient scale may vary considerably with the underlying CDR technology. Let $v(k)$ denote the upfront capital expenditure for a plant capacity capable of capturing and sequestering k tons of CO_2 in any given hour. The corresponding annual fixed operating costs are denoted by $f_i(k)$. Variable operating costs, which include the transport and storage of the captured CO_2, are assumed to be an increasing function $w_{it}(\cdot)$ of q_{it}. In the context of DAC, for instance, the cost of purchased electricity is the main driver of variable costs and this cost will generally vary across the hours of any given year.

The operating costs of the facility may be offset by *co-product* revenues. In the context of BiCRS or ERW, such co-product revenues may reflect the sale of biochar or other agronomic yield benefits, respectively. For BECCS plants, electricity sales constitute, by definition, a major co-product revenue stream. Since the magnitude of the revenues will frequently vary with the real-time wholesale prices for electricity, we represent the co-product revenues by a time-dependent function $CPR_{it}(\cdot)$. Co-product revenues also include production tax credits such as those specified in connection with Section 45Q of the U.S. tax code.

We refer to the entire vector of life cycle sequestration quantities q_{it}, for $1 \leq t \leq m$ and $1 \leq i \leq T$, as a utilization schedule and represent this vector by $\vec{q}$. Suppose the investor receives a carbon credit of p dollars per net ton of CO_2 sequestered. Future cash flows are discounted with the per-period factor $\gamma = \frac{1}{1+r}$, where the cost of capital r is interpreted as the weighted average cost of capital (WACC). The discounted future cash flows to the investor are thus given by:

$$DCF^o(p, \vec{q}) = \sum_{i=1}^{T} \left[\left(\sum_{t=1}^{m} \left(p \cdot (1-\alpha) \cdot q_{it} + CPR_{it}(q_{it}) - w_{it}(q_{it}) \right) \right) - f_i(k) \right] \gamma^i - v(k). \quad (1)$$

If the investment is made by a regular for-profit corporation, the LCCDR break-even criterion must be applied in terms of after-tax cash flows. To that end, let τ denote the corporate income tax rate. If the initial capital investment, $v(k)$, can be depreciated over its useful life according to a schedule $d = (d_1, d_2, \ldots, d_T)$, with $\sum_{i=1}^{T} d_i = 1$, the company's taxable income in year i, $I_i(p, \vec{q})$, is given by its cash flow in that period less the applicable depreciation charges (see Methods for details). The life-cycle after-tax cash flows then amount to:

$$DCF(p, \vec{q}) = DCF^o(p, \vec{q}) - \sum_{i=1}^{T} \tau \cdot I_i(p, \vec{q}) \cdot \gamma^i. \quad (2)$$

The levelized cost of carbon dioxide removal, LCCDR, is defined as the lowest price, p, that allows investors to earn their required rates of return by breaking even in terms of discounted after-tax cash flows. An implicit assumption for this break-even criterion is that the plant in question is utilized efficiently subject to its feasibility constraints. In general, it may not be efficient for the available capacity to always be fully utilized. Similar to natural gas plants that do not profit from generating electricity during hours of low power prices, a

BECCS plant may, depending on the price p for carbon credits, be better off not to operate the plant during hours of low electricity prices. The maximized discounted stream of future cash flows is given by:

$$DCF^*(p) = \max_{\vec{q} \in F} DCF(p, \vec{q}) \equiv DCF(p, \vec{q}^{\,*}(p)), \tag{3}$$

where F denotes the set of feasible utilization schedules and $\vec{q}^{\,*}(p)$ denotes the value-maximizing utilization schedule, given p. The LCCDR therefore is the lowest price, p that would allow investors to break even that is, it solves $DCF^*(p) = 0$. Although the equation,

$$DCF^*(\cdot) = 0$$

is non-linear in p, it is shown in Methods that the expression for $DCF(p, \vec{q})$ exhibits sufficient separability so as to ensure a unique solution. This finding relies on the plausible assumption that investors could not possibly already break even if carbon credits had no market value.

Claim: *Suppose* $DCF^*(p = 0) < 0$*. Then there is a unique value* $LCCDR > 0$ *such that* $DCF^*(LCCDR) = 0$.

Our analysis below finds a considerable range of LCCDRs for the four alternative CDR technologies considered in this study. To highlight the impact of both leakage and co-product revenues on the LCCDR, we also calculate two variant levelized cost metrics. By $LCCDR^+$ we denote the levelized cost metric that obtains if one drops all co-product revenues, that is, both co-product sales and policy credits. By definition, $LCCDR^+ \geq LCCDR$. In contrast, $LCCDR^-$ denotes the levelized cost metric that obtains if offsetting Scope 1 and 2 emissions are considered negligible, that is, $\alpha = 0$. Examining the latter metric is of particular interest since different off-take agreements for carbon removals may apply different system boundaries in accounting for offsetting emissions.

3 Alternative Carbon Removal Technologies

The four CDR technologies examined here differ primarily in how carbon is captured and stored. Figure 3 illustrates the monetary and carbon flows associated with a generic removal facility. BECCS, as described above, captures biogenic CO_2 from flue gas and stores it underground. BiCRS stores biogenic carbon in durable biomass products such as bio-oil and biochar. DAC captures CO_2 from the ambient air for geological storage. ERW removes atmospheric CO_2 through mineral weathering and stores it in dissolved or solid inorganic forms.

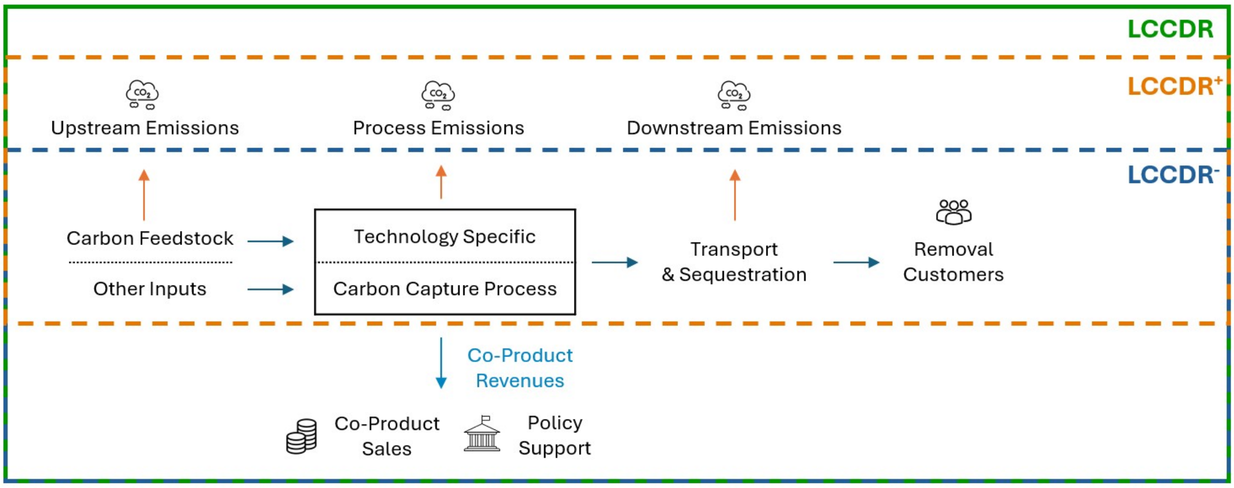

Figure 3. Generic carbon removal process. This figure illustrates the techno-economic setting generalized to all removal technologies considered. Our base LCCDR calculation presumes system boundaries that account for all emission and revenue sources inside the green box. Upstream, process, and downstream emissions are reflected in the endogenous parameter α, while co-product sales and applicable policy support are reflected in CPR. The blue and orange boxes show the no-leakage LCCDR$^-$ and no-revenue LCCDR$^+$ levelized costs, respectively.

3.1 Bioenergy with Carbon Capture and Storage (BECCS)

Bioenergy with carbon capture and storage (BECCS) is among the most commercially mature of the four pathways[68]. A representative facility combusts pulverized biomass in a boiler for combined heat and power and routes the flue gas through an amine-based post-combustion capture unit. Capture rates of about 90% are standard, as higher rates incur disproportionately increasing cost[69]. The captured stream is compressed, transported, and injected into geological storage. BECCS provides dispatchable low-carbon electricity alongside removal credits[70].

In the notation of our Economic Model, the sequestered quantity q_{it} is the gross CO_2 captured and delivered to durable storage. Variable operating costs are dominated by the delivered biomass price and depend on the biomass feedstock type. Biomass takes up atmospheric CO_2 as it grows. Capturing and sequestering this CO_2 leads to negative emissions, i.e. a removal. In our main analysis, we use a biogenic-neutral convention. Under this convention, biogenic carbon released during conversion is balanced out by biomass regrowth. As we mainly consider residual biomass, the presumption is that this biogenic CO_2 would otherwise be released to the atmosphere sooner or later. Consequently, uncaptured flue gas emissions during the capture process are not counted as an offsetting emission. The leakage factor α therefore comprises the upstream feedstock emissions (harvesting, processing, and transport), together with downstream emissions incurred during transport and storage of CO_2. We further do not consider any avoided emissions, such as methane released by residue decomposition. We discuss the impact of including uncaptured biogenic emissions and potential land-use-change emissions in Supplementary Note 4.

Co-product revenues comprise electricity sales and the 45Q tax credit. The base case values electricity at an annual-average wholesale price. An hourly-price check yields a similar net removal cost. The calibration draws on recent techno-economic studies of biomass-fired generation with amine capture and on observed U.S. electricity and biomass prices (see Methods for details on model configuration, inputs and supplementary checks).

Various challenges arise for BECCS deployment in practice. First, net removals require reliable quantification of upstream biomass carbon content and supply-chain emissions[44]. Second, the cost advantage of residue-based projects depends on a reliable feedstock supply. Fire, pests, competing demand, and rising feedstock prices can reduce availability or raise delivered cost[68;71–73]. Geological storage may also require continued costly monitoring[74].

3.2 Biomass Carbon Removal and Storage (BiCRS)

Biomass carbon removal and storage (BiCRS) converts biomass into stable carbon products via pyrolysis, the thermochemical conversion of organic matter under oxygen-limited conditions at high temperatures[75;76]. Pyrolysis produces three major outputs: a solid fraction (biochar), a liquid fraction (bio-oil), and a gaseous fraction (syngas). In practice, pyrolysis is highly adaptable and can utilize a broad spectrum of feedstocks, including woody biomass, agricultural residues, sewage sludge, and even non-biomass wastes[77–80]. Feedstock type, along with process parameters such as heating rate, temperature, residence time, and reactor configuration, strongly influences the yield distribution between biochar, bio-oil, and syngas[81;82]. In our baseline modeling, we focus on slow pyrolysis, which typically yields around 35% biochar, 30% liquids, and 35% syngas by mass[83].

Applying the Economic Model to BiCRS requires an additional conceptual step because no direct CO_2 stream is captured. We count as gross sequestration q_{it} the biogenic carbon fixed in the two durable product streams converted to CO_2e (at the molar mass ratio 44/12). This includes the biochar carbon that remains stable over at least a 100-year horizon, and the bio-oil carbon destined for geological injection. We apply a permanence factor of 80% to the biochar carbon, at the conservative end of estimates[84;85]. Injected bio-oil is counted in full. The syngas fraction is combusted on site to supply process heat. Under the same biogenic-neutral convention as for BECCS, this release is not counted as an offsetting emission. The leakage factor α includes emissions from feedstock harvesting and truck transport, grid electricity for plant operation, and biochar distribution. We neither credit avoided residue decomposition nor include indirect land-use-change emissions in the main analysis; the alternative boundaries are reported in Supplementary Note 4.

The calibration combines techno-economic inputs with woody-residue prices and transport distances for the U.S. Southeast. Co-product revenue is the sale of physical biochar as a soil product, which is separate from the removal-credit price p. The geological storage of bio-oil contributes to removal but is not a saleable co-product itself. Principal uncertainties are the biochar permanence factor, feedstock cost and availability, and the physical biochar sales price (see Methods for model configuration, inputs, and supplementary checks). We also test a credit-eligibility boundary in which biochar is sold as a co-product, but not eligble to earn removal credits. If only injected bio-oil is credited, this raises the break-even price per net ton considerably (see Supplementary Note 4.4).

Several challenges complicate assessing BiCRS economics in practice. Published literature estimates are difficult to compare when they use different feedstocks, reactor designs, functional units, or permanence conventions[86;87]. We hold the slow-pyrolysis process and accounting convention fixed and vary feedstock and logistics explicitly. This matters because low-density or wet biomass becomes costly to transport over long distances, which can favor smaller plants located near the feedstock source[88;89].

3.3 Direct Air Capture (DAC)

The process of capturing CO_2 from ambient air involves two main parts: the air contactor and the regeneration unit. In the first stage, atmospheric air is brought into contact with a chemical capture material, where CO_2 is bound by the material. In the second stage, the

CO_2 is released and captured, while the capture material is regenerated[62]. The two main technologies available are characterized by the chemical processes used to capture the carbon: solid sorbents (S-DAC) and liquid solvents (L-DAC)[90]. L-DAC uses an aqueous hydroxide solution (such as KOH), from which the CO_2 is later released via a high-temperature calcination process[63]. S-DAC on the other hand captures CO_2 using sorbents such as amine-based materials, which then release the carbon via a thermal swing or vacuum swing process[90].

According to our Economic Model, q_{it} is the gross CO_2 captured at the DAC plant and delivered to durable storage; capture, transport, and injection are synchronized. The base grid configurations use an annual, location-based Scope 2 accounting method: purchased electricity is assigned the regional grid carbon intensity. The renewable-coupled configurations instead use the modeled project supply mix, including retained grid backup. Purchased energy consequently dominates α, alongside smaller transport-and-storage emissions. L-DAC also uses natural gas for high-temperature calcination. Under current grid supply, these inputs place DAC among the highest-leakage base cases, while dedicated low-carbon energy lowers α. Capacity cost is the largest cost component, followed by variable operating costs. DAC has no marketable co-products. Its only offsetting revenue is the 45Q tax credit, making it the only technology whose co-product revenue is entirely policy-dependent.

The calibration relies on recent techno-economic studies, manufacturer estimates and U.S. data (see Methods for details on model configuration, inputs and supplementary checks). Current DAC economics are less favorable than those of other technologies and reported costs vary widely with the underlying assumptions. Principal uncertainties include future capital cost and energy requirements. Meanwhile, realized performance depends critically on the carbon intensity of the energy supply and feasible operating conditions[91–94]. We do not model land-use requirements for DAC, which are unlikely to be a binding constraint relative to other removal pathways at scale[95].

3.4 Enhanced Rock Weathering (ERW)

ERW refers to a geochemical process that relies on natural weathering to capture CO_2 from the atmosphere[18]. This can be engineered by spreading finely crushed silicate rocks on land surfaces, for instance agricultural soils[49]. The approach has gained recent attention due to its potentially low cost, compatibility with existing land use, high scalability and durability[52;56;96]. A practical advantage of ERW is its compatibility with existing agricultural logistics: crushed rock can often be applied with equipment already used for liming and fertilizer distribution, limiting the need for new downstream infrastructure[49;50]. Silicate dissolution also releases base cations and nutrients such as calcium, magnesium, and potassium, which may improve soils and yields[50;52].

The essence of ERW is that CO_2 dissolves in water to form carbonic acid, which then reacts with silicate minerals in crushed rocks. Silicate weathering releases base cations and generates bicarbonate. The inorganic carbon may be transported toward the ocean or retained in soils as secondary carbonate minerals. These end states can store carbon durably, but realized permanence depends on transport pathways, secondary reactions, and the ability to verify the retained carbon[97–99]. Weathering rates depend on mineral type and composition, particle size, and environmental conditions[49]. We model basalt and dunite as cases in point, which exhibit two trade-offs. Dunite can weather faster and absorb more CO_2 per ton of rock, whereas basalt is more abundant and avoids concerns on nickel and chromium release from ultramafic minerals[49;55]. Finer grains generally increase reactive surface area and gross removal potential but also raise grinding cost, electricity use, and upstream emissions[56;99].

To adapt our modeling framework to ERW, let z_{it} denote the number of tons of a particular type of rock that is being processed (ground) and transported to its destination in hour t of year i. We suppose that in year $i+j$ each ton of rock absorbs (sequesters) μ_j tons of CO2 from the ambient air. The sequence of μ_j is decreasing and approaches zero over time. The total discounted tons of CO2 sequestered through processing z_{it} tons of rock then becomes:

$$q_{it} = z_{it} \cdot \sum_{j=0}^{\infty} \mu_j \cdot \gamma^j.$$

In our main calibration, we set $\mu_0 = \omega \cdot Y^{\max}$, where ω is the assessed annual dissolution fraction and $Y^{\max}$ is the rock-specific CO_2-uptake ceiling per ton of rock, and assume for simplicity

$$\mu_j = \omega \cdot (1-\omega)^j \cdot Y^{\max}.$$

The main case credits only the CO_2 uptake expected during the application year, i.e. $q_{it} = z_{it} \cdot \mu_0$. This is because field weathering rates and the verification of residual uptake remain uncertain. Theoretical and laboratory-derived rates may overstate field performance, and some mineral fractions may remain effectively unweathered within a project-relevant horizon[50;55;99;100]. The convention is also in line with current verification practice, under which registries credit ERW ex post for weathering measured after application[101;102]. Crediting verified residual uptake beyond the application year, such as in steady-state assessments[55], would raise removal per ton of rock and lower LCCDR. Supplementary Note 7 reports this alternative and tests the impact of slower field weathering, different grain sizes and MRV costs.

After spreading, ERW has no separate transport-and-storage step. Since ERW (currently) receives no policy support, co-product revenue is limited to the value of a small agricultural co-product for basalt. This premium is not available for dunite, given its trace-metal concerns. The leakage factor α includes mining, grinding, transport, and field application. Grinding electricity dominates basalt emissions and links its grain-size choice directly to both cost and leakage. Dunite's higher reactivity permits a coarser grind, leaving transport as its largest attributable emission source.

The basalt application settings draw on field-trial evidence, whereas the weathering rates at the assumed grain sizes for both rocks rely mainly on laboratory and modeled bounds[50;55;56] (see Methods for details on model configuration). Whether these rates are realized in heterogeneous field soils remains uncertain. For dunite, trace-metal risks further constrain suitable application sites[99]. Verification cost can also be material because credited uptake must be separated from background soil and hydrological variation[51;100;103;104].

4 Results

4.1 Base Case Results

For each of the four CDR technologies considered in our analysis, this subsection reports levelized cost estimates for a base case in the context of the U.S. market and regulatory environment. BECCS Wood and BiCRS Wood use woody residues as feedstock. S-DAC Grid and L-DAC Grid use electricity from the commercial grid. ERW Basalt and ERW Dunite evaluate facilities that grind and apply basalt and dunite rock, respectively.

Across our numerical calibrations, it is financially advantageous to use the full practical capacity k, so that $q^*_{it} = k$. Specifically, we verified that a DAC facility yields a positive contribution margin even during hours when power prices are high, in part because of the sizable production tax credits available. Similarly, the combination of production tax credits and removal-credit revenue at the break-even price makes it advantageous to run a BECCS plant even during hours with low electricity prices. Supplementary Note 5 provides details.

Provided $q^*_{it} = k$, the LCCDR can be expressed as the sum of the levelized capacity cost c and the fixed and variable operating costs f and w, less the levelized co-product revenue CPR. Formally,

$$LCCDR = c + f + w - CPR,$$

where the four levelized components, stated per net ton removed, are defined as:

$$c = \frac{v(k)\Delta}{(1-\alpha)L}, \qquad f = \frac{\sum_{i=1}^{T} f_i(k)\gamma^i}{(1-\alpha)L}, \qquad w = \frac{\sum_{i=1}^{T}\sum_{t=1}^{m} w_{it}(k)\gamma^i}{(1-\alpha)L},$$

$$CPR = \frac{\sum_{i=1}^{T}\sum_{t=1}^{m} CPR_{it}(k)\gamma^i}{(1-\alpha)L}.$$

The levelization factor $L \equiv m \cdot k \cdot \sum_{i=1}^{T} \gamma^i$ represents the total discounted processing capacity of the facility. The tax factor $\Delta = (1 - \tau \sum_{i=1}^{T} d_i \gamma^i)/(1-\tau)$ reflects the corporate income tax rate τ and depreciation schedule $(d_1, \ldots, d_T)$. CPR includes physical co-product sales and applicable tax-adjusted policy support.

To highlight differences in the cost structure of the four CDR technologies, we report each of the three cost components per net ton. To further examine the impact of leakage and co-product revenues, the following Table 1 also shows the two variant levelized cost figures that obtain if either leakage is ignored or co-product revenues are not available, namely:

$$LCCDR^- = LCCDR \cdot (1-\alpha) \quad \text{and} \quad LCCDR^+ = LCCDR + CPR.$$

Figure 4 provides a graphical representation of the four cost and co-product revenue components shaping the levelized cost metrics we examine.

We find that ERW Dunite has the lowest base-case LCCDR, while S-DAC Grid has the highest, just over ten times as high. S-DAC combines the highest capacity cost with electricity-intensive operation. Its variable operating cost is almost twice that of L-DAC. While both configurations require electric and thermal inputs, L-DAC requires substantially more thermal energy, supplied by natural gas rather than electricity. This lowers costs but can lead to increased attributable emissions. Meanwhile S-DAC requires more electricity and expensive sorbents that degrade faster, despite lower thermal requirements. BECCS

Metric ($/tCO$_2$)	BECCS Wood	BiCRS Wood	S-DAC Grid	L-DAC Grid	ERW Basalt	ERW Dunite
Capacity cost (c)	84.7	48.1	401.1	307.3	4.4	1.0
Fixed operating cost (f)	28.4	18.1	121.1	103.8	97.7	21.7
Variable operating cost (w)	82.5	72.5	274.2	138.1	177.5	25.1
Leakage (α)	4.60%	5.22%	34.16%	32.61%	32.28%	3.92%
Co-product Revenue ($-CPR$)	−106.3	−31.6	−304.7	−259.5	−19.3	0.0
LCCDR$^-$	85.3	101.5	323.7	195.2	176.3	45.9
LCCDR	89.4	107.1	491.7	289.6	260.3	47.8
LCCDR$^+$	195.7	138.6	796.4	549.1	279.6	47.8

Table 1. LCCDR comparison across base configurations. The table reports the six current U.S. base configurations. Cost and revenue components are shown per net ton of CO_2 removed. The three LCCDR metrics are measured per ton of CO_2 removed under their respective system boundaries. The capacity cost incorporates applicable taxes and depreciation allowances. Variable operating cost includes transport and storage charges.

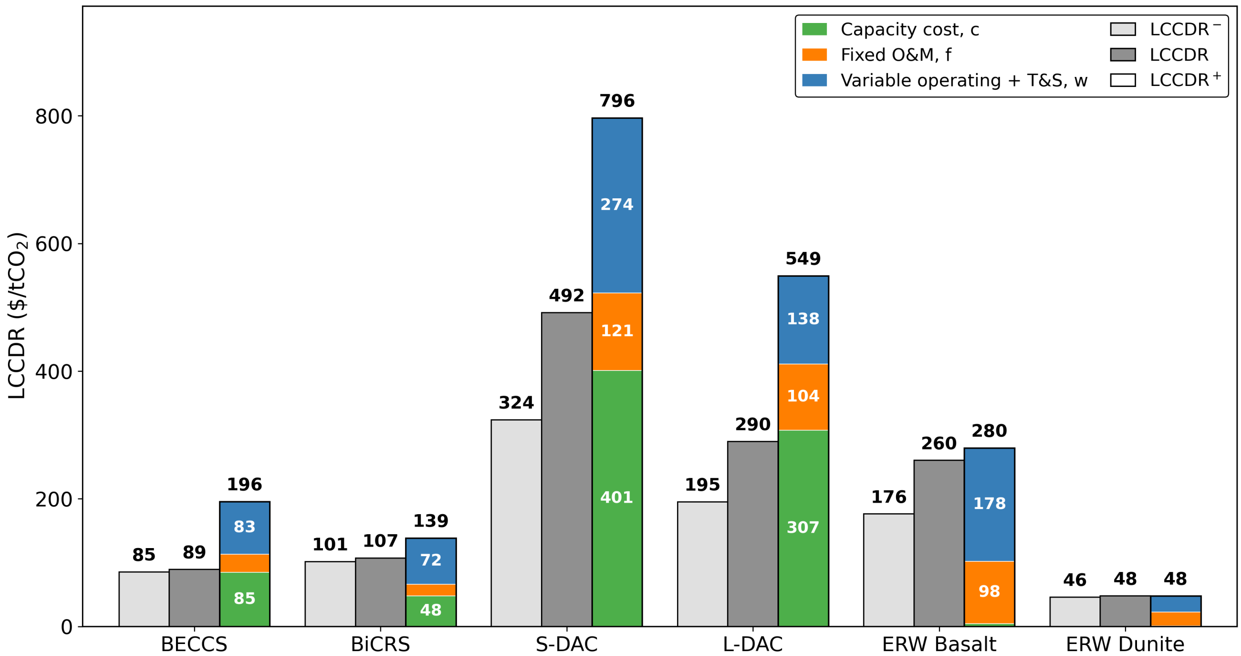

Figure 4. LCCDR and cost composition across base configurations. The bars show the transition from LCCDR$^-$ to LCCDR and then to LCCDR$^+$. The LCCDR$^+$ bar separates capacity cost, fixed operating cost, and variable operating cost including transport and storage. The drop from LCCDR$^+$ to LCCDR shows the effect of co-product revenue and policy support.

has a higher plant-gate cost than BiCRS, but electricity revenue and 45Q lower its investor break-even price considerably.

For the biomass pathways, revenue reverses the cost order of the base cases. Before co-product and policy revenue, BECCS costs 41% more than BiCRS, but it receives a \$106/tCO_2 offset from electricity sales and 45Q, more than three times the \$32/tCO_2 physical biochar revenue in BiCRS. Its resulting investor break-even price falls to \$89/tCO_2, about 17% below the \$107/tCO_2 BiCRS estimate. BECCS is therefore cheaper in the main metric because of its co-product revenue.

The basalt–dunite difference instead comes from physical removal yield and processing energy. Basalt requires a 7 µm grind in the base case, compared with 30 µm for dunite, and removes less CO_2 per ton of rock. Its variable cost is consequently about seven times higher (\$178 versus \$25/tCO_2). Dunite remains the least-cost base case even without co-product revenue, but this result relies on the achievable weathering rate and suitable application sites.

In terms of leakage, we find that attributable emissions are driven by different inputs. Purchased energy dominates attributable emissions for DAC and basalt ERW, whereas feedstock preparation and transport dominate BECCS and BiCRS under the biogenic neutral convention. Downstream transport and storage losses add comparatively little. The resulting leakage factor is 32–34% for S-DAC Grid, L-DAC Grid, and ERW Basalt, compared with 4–5% for BECCS Wood, BiCRS Wood, and ERW Dunite. Because 45Q is paid per gross ton, this leakage also changes its effective value per net ton. For the DAC base cases, the credit reduces the investor break-even price relative to LCCDR^+ by 38% for S-DAC and 47% for L-DAC. This is a direct consequence of gross-ton crediting. We report the corresponding values without 45Q in Supplementary Note 2.

4.2 Alternative Project Configurations

The base case configurations can provide one plausible reference per technology, but they do not represent the full range of current project economics. We therefore evaluate twelve alternative configurations to complement the base cases. A project configuration induces a complete set of technical, energy, supply-chain, and financial assumptions. For each technology the configurations are labeled by their defining choice. Frontier-DAC is a current 0.1 MtCO_2/yr early plant, using grid electricity and upper-bound current capital costs. Commercial-Grid is a 1 MtCO_2/yr plant with base capital costs and grid electricity. Renewable-

Coupled retains the Commercial-Grid plant architecture and scale but changes the electricity supply to co-invested wind and solar with grid backup. BECCS and BiCRS configurations vary feedstock and logistics parameters. The ERW Favorable, Realistic, and Conservative configurations jointly vary electricity supply, grain size, transport distance, and agronomic revenue. Together, the alternative configurations show how feasible choices impact cost and leakage profiles. Full details on model calibrations are provided in Methods.

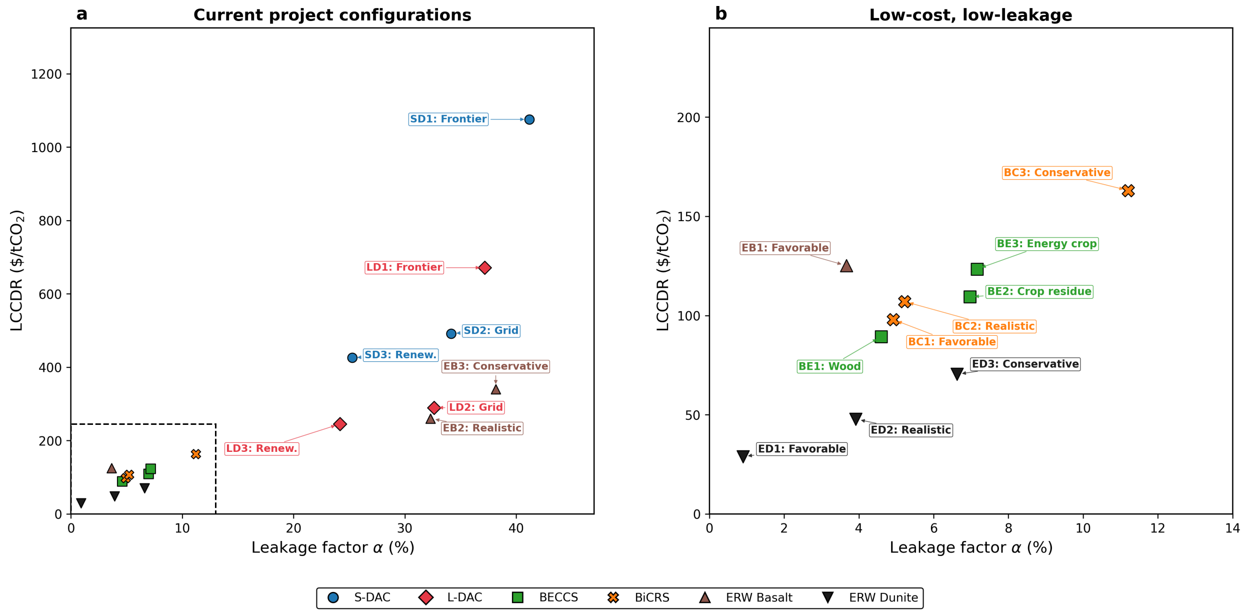

Figure 5. LCCDR and leakage across project configurations. Panel (**a**) shows the full comparison. Panel (**b**) enlarges the low-cost, low-leakage region.

Figure 5 shows the relationship between α and LCCDR across the project configurations. The configurations occupy three broad regions. Dunite ERW forms a modeled low-cost, low-leakage frontier. The biomass configurations and Basalt-Favorable have low leakage at moderate cost. DAC and the more energy-intensive basalt configurations have both higher cost and higher leakage. Across these groups, energy supply shapes the DAC and ERW outcomes, while feedstock sourcing shapes the biomass pathways.

Figure 6 shows how these configuration choices shift the LCCDR outcomes. The LCCDR range is widest for S-DAC (\$426–\$1,076/tCO$_2$) and lowest for Dunite ERW (\$29–\$70/tCO$_2$). The S-DAC range is widest because the Frontier plant is smaller and assumes higher capital costs. Frontier LCCDR is 119% higher than Commercial-Grid for S-DAC and 132% higher for L-DAC. Renewable coupling lowers LCCDR by 13% for S-DAC and 15% for L-DAC relative to the base case. For S-DAC, that translates into \$65.9/tCO$_2$, \$8.4 from lower

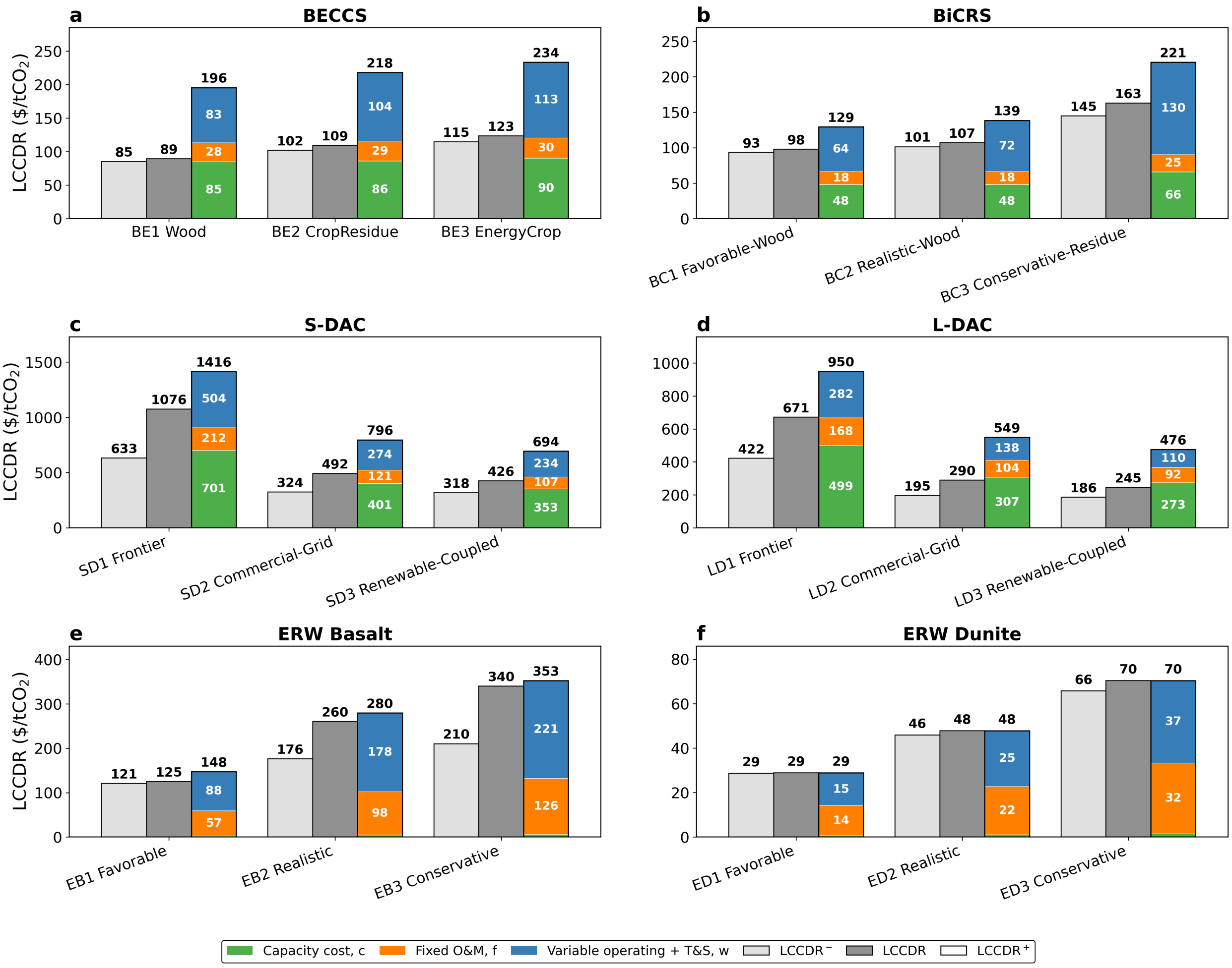

Figure 6. LCCDR comparison across project configurations. Each panel (**a**) through (**f**) shows three configurations for one technology. The three bars for each configuration report LCCDR^{-}, LCCDR, and LCCDR^{+}, as introduced above.

electricity cost and \$57.5 from the lower leakage factor. For L-DAC, this means a reduction of \$44.5/tCO_2, \$13.8 via lower energy cost and \$30.7 from lower leakage. The leakage factors fall by 8.9 and 8.4 percentage points, respectively. Cleaner energy therefore leaves a larger share of gross sequestration as net removal and lowers cost per net ton. These estimates already include the countervailing effect that a lower α reduces the effective per-net value of the 45Q tax credits.

In the BECCS configurations, using the energy crop miscanthus as feedstock is costlier and more emissions-intensive than woody residues. Longer transport distances have a similar effect. Replacing woody residues with miscanthus raises BECCS LCCDR by 38% and α by 2.6 percentage points. For BiCRS, replacing wood chips with corn stover and extending the haul raises LCCDR by 52% and α by 6.0 percentage points. Co-product revenue changes little across the BECCS configurations because they use the same electricity-price and 45Q assumptions. Their cost differences are therefore driven mainly by delivered feedstock cost and upstream emissions. The dedicated-energy-crop result is also sensitive to the land-use boundary. A 10 gCO_2e/MJ grassland-conversion penalty would raise the BECCS energy-crop configuration from \$123 to \$143/tCO_2, while a 50 gCO_2e/MJ cropland debit raises it to \$401/tCO_2. At approximately 72 gCO_2e/MJ, the configuration no longer delivers net removal (see Supplementary Note 4.3). The removal-credit boundary is equally important for BiCRS. If only bio-oil were to be carbon credit-eligible and biochar only a co-product, the required credit price more than doubles: for Realistic-Wood it increases from \$107 to \$231 per net credited ton (see Supplementary Note 4.4).

Basalt ERW spans \$125–\$340/tCO_2 and leakage factors of 3.7–38.2%, the widest leakage range among the configurations. This range reflects joint changes in electricity supply, target grain size, transport distance, and agronomic revenue. The largest gap separates the renewable-powered Basalt-Favorable configuration from the more grid-dependent configurations because fine basalt grinding is electricity-intensive. Dunite remains in a narrower range of 0.9–6.6% leakage and \$29–\$70/tCO_2, mainly because its higher modeled uptake permits coarser grinding and lower variable operating costs. These estimates require suitable land and depend on whether the modeled weathering rates at the assumed grain sizes are achieved in the field. Field verification may also entail additional site-specific MRV costs. Powering the grinding with clean electricity lowers the Basalt-Realistic LCCDR from \$260 to \$192/tCO_2 and α from 32% to 8%, but changes Dunite-Realistic by less than \$1/tCO_2. Extending the horizon over which modeled uptake can be reliably verified from one to five years lowers the two base estimates from \$260 to \$172 and from \$48 to \$31/tCO_2, respectively. In separate one-at-a-time checks, Dunite-Realistic remains below \$100/tCO_2 when realized field weathering falls to 50% of the modeled rate. At an adjustment rate of 0.35 for more temperate climates, it raises the estimate to \$148/tCO_2. These sensitivities point to an important issue for multi-year projects, namely how to reliably measure field-performance and who carries the verification risk (see Supplementary Note 7).

Taken together, the results do not indicate a universal trade-off between cost and leakage. Technology determines the broad cost range, while energy supply, feedstock, logistics, and scale affect where individual projects lie within the cost–leakage space. Technology labels alone are therefore insufficient for comparing projects, underscoring the importance of project-specific disclosures.

4.3 Cost Estimates versus Market Prices

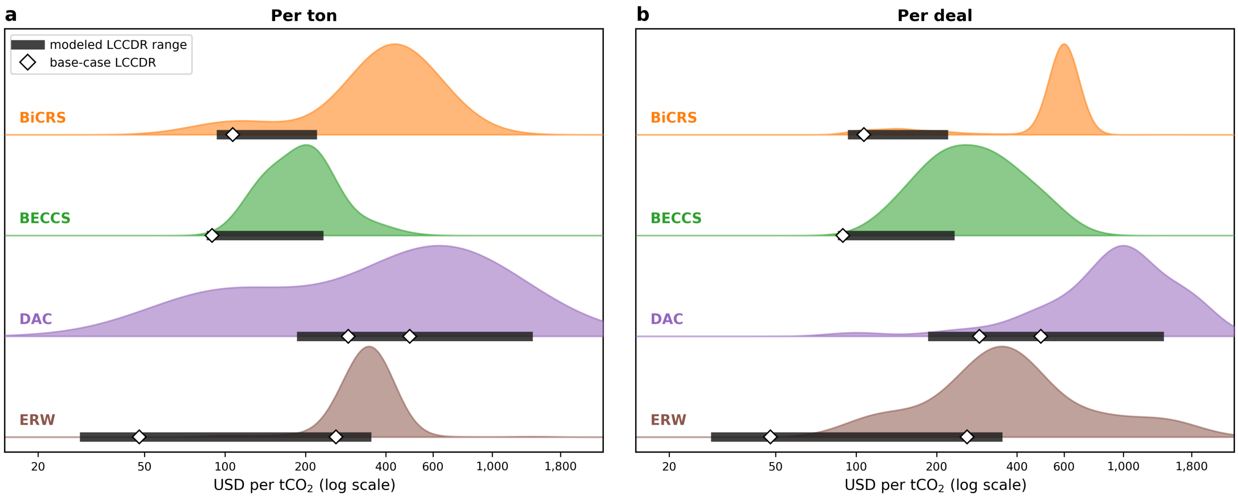

Figure 7. Observed transaction prices and modeled removal costs. This figure shows the distribution of observed prices by pathway on a log scale. Panel (**a**) weights each transaction by contracted tonnage, while panel (**b**) gives each transaction equal weight. The dark horizontal bars span the modeled range from the lowest $LCCDR^-$ to the highest $LCCDR^+$ across current project configurations. White diamonds mark the base-case LCCDR values. Source: CDR.fyi[19].

Observed transaction prices provide a point of comparison with our modeled results, but prices can include scarcity rents, risk premia, contracting services, and other items that are absent from our estimates. Figure 7 compares each pathway's modeled LCCDR range with disclosed transaction prices in CDR.fyi[19]. We distinguish between a tonnage-weighted distribution in panel (a) and an unweighted, per-deal distribution in panel (b) to show how large contracts influence the overall price distribution (see details in Supplementary Note 2.1).

We find that most disclosed BECCS and DAC prices fall within their modeled ranges. The tonnage-weighted median is about \$214/tCO_2 for BECCS and \$650/tCO_2 for DAC. The BiCRS median of about \$382/tCO_2 exceeds the modeled upper bound of \$221/tCO_2, influenced by one large biochar transaction and a bio-oil segment priced mainly by one supplier. The ERW median of about \$368/tCO_2 lies just above its modeled upper bound of \$353/tCO_2 and far above the dunite range. These gaps may reflect verification cost and risk, delivery risk, supplier concentration, scarce supply, or contract-specific services. For both DAC and BiCRS, giving each deal equal weight shifts the distribution toward higher prices than in the tonnage-weighted panel. Larger contracts therefore tend to exhibit lower per-ton prices than smaller contracts within the same pathway. In BiCRS, this contrast is especially visible in the many smaller biochar and bio-oil transactions. The pattern is consistent with volume discounts or other structural differences between large and small contracts.

The input sensitivity checks show how much of these gaps model-input uncertainty may explain. Sensitivity ranges result in cost changes -19% to $+37\%$ for BECCS Wood and -15% to $+24\%$ for BiCRS Wood. Both thereby remain below their observed median prices (\$72–\$123 to \$214/tCO_2 and \$91–\$133 to \$382/tCO_2). DAC and ERW Basalt medians lie at or within their sensitivity ranges. The biomass price–cost gaps therefore cannot only be attributed to different project cost parameters alone (see Supplementary Note 3).

5 Discussion and Conclusion

Our comparison considers three cost measures that are frequently mixed in removal decisions. These metrics separate the investor break-even price from the effects of attributable emissions, co-product revenue, and policy support. Our main results reveal a 37-fold range in current investor break-even prices, from \$29/tCO_2 for the Dunite-Favorable ERW configuration to \$1,076/tCO_2 for Frontier S-DAC, and leakage factors from 1% to 41%. These ranges reflect both technology maturity and project configurations. Cost estimates that ignore attributable emissions, LCCDR$^-$, can understate full net removal costs LCCDR by as much as 70%. Co-product revenue and policy support can lower LCCDR by 0–54% relative to the revenue-free LCCDR$^+$.

Adding cleaner input sources lowers leakage without necessarily increasing total cost. Decarbonizing energy supply and upstream logistics can thereby improve removal economics even in cases where the cleaner options are more expensive per unit cost. There are also cases without such a trade-off: In suitable geographies, co-invested wind and solar can lower both variable energy cost and upstream emissions. Procurement and policy that reward clean-power coupling can therefore improve cost and net removal simultaneously. Cleaner electricity is especially important for DAC and basalt grinding. Dunite is less sensitive because grinding accounts for a smaller share of its cost and emissions.

The current results also indicate how costs may change in the future. DAC has the clearest potential for experience-curve learning because repeated deployment can reduce equipment and fixed operating costs[17;22]. We model prospective DAC costs over various future configurations. On the policy-free LCCDR$^+$ measure, S-DAC is estimated to fall from \$796/tCO_2 in the current Commercial-Grid case to \$182/tCO_2 in the long-term 2050 case, while L-DAC falls from \$549 to \$207/tCO_2. These values combine equipment learning with changes in process performance, energy supply, project lifetime, and transport-and-storage scale. None of the modeled DAC configurations reaches the U.S. Carbon Negative Shot target of \$100 per net ton. The Mature-2030 configurations reach \$111–\$135/tCO_2 with 45Q but cost \$313–\$366/tCO_2 without it. Even the policy-free long-term 2050 configurations remain at \$182–\$207/tCO_2. Both learning and continued policy or market revenue would therefore be needed to approach the target. Future biomass economics depend mainly on feedstock markets and logistics, while cleaner grinding electricity is the central dynamic examined for ERW. The future DAC configurations and cleaner-grid ERW scenarios are reported in Supplementary Note 6.

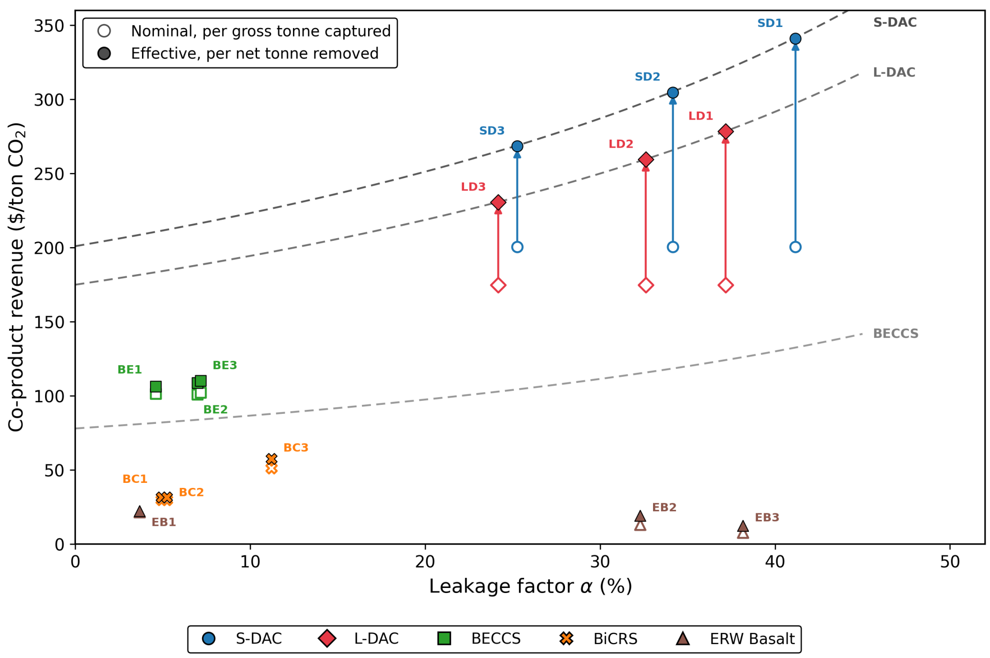

Figure 8. Leakage and the net value of co-product revenue. The curve converts nominal revenue per gross ton to its effective value per net ton, defined as CPR. Dashed lines show levelized, tax-adjusted 45Q values. Points show total co-product and policy revenue for each base configuration. BECCS also includes electricity revenue, while BiCRS and ERW only reflect biochar sales and agronomic yield revenue.

Tax-credit design matters most for DAC and BECCS. Figure 8 shows the relationship between leakage and the effective per-net value of gross-ton revenue. The levelized, tax-adjusted 45Q credit is worth \$78–\$201 per gross ton. Allocating it over the smaller quantity of net removal raises its effective value to \$82–\$341 per net ton. Because 45Q pays for gross sequestration, it does not directly reward reductions in attributable emissions. Our calculations do not imply that investors will deliberately select higher-emission inputs. Project configuration choices will mainly depend on input costs, credit revenues, and feasibility. But our results show that a gross-ton credit provides no incentive for reducing attributable emissions. At a fixed credit rate, a higher-α project therefore delivers fewer net tons per tax dollar spent. Paying for independently verified net removal would strengthen the reward for reducing α, aligning support more closely with net-removal outcomes. Policy support also changes the cost ranking. Without 45Q, BECCS Wood rises from \$89 to \$171/tCO_2 and no longer undercuts BiCRS Wood at \$107/tCO_2 (see Supplementary Note 2). Under current law, projects must begin construction before 2033 to qualify for the credit[14], which limits its role in long-run economics. Time-limited credits can support early scale-up but may not suffice if the credit expires before the technology achieves commercial viability.

Several limitations bound the interpretation of our results. First, absolute costs remain sensitive to input assumptions. Parameter checks identify DAC capacity utilization and plant cost, biomass plant and feedstock cost, and ERW grain size and removal yield as the main cost drivers (see Supplementary Note 3). Second, biomass results depend on accounting and eligibility rules. We neither credit avoided residue decomposition nor assign a land-use-change penalty because neither counterfactual can be observed for the contracted feedstock. Counting uncaptured biogenic CO_2 as an offsetting emission raises Conservative-Residue BiCRS α from 11% to 38% and LCCDR from \$163 to \$234/tCO_2. Restricting eligibility to bio-oil only raises its required credit price to \$354 per net credited ton (see Supplementary Note 4.4). Third, the main ERW estimates use 25 °C reference weathering rates and credit only application-year uptake. Extending verified crediting from one to five years lowers the two realistic-configuration estimates by about one-third. By contrast, applying a lower temperate weathering factor can raise the dunite range roughly threefold, from \$29–\$70 to \$84–\$232/tCO_2. Under the same adjustment, Basalt-Realistic would get prohibitively expensive and Basalt-Conservative net-emitting. Slower field realization and declining marginal effectiveness under repeated applications would also raise costs. Supplementary Note 7 elaborates on alternative weathering rates, grain sizes, crediting horizons, and MRV costs. Our calibrations are U.S.-anchored, and rankings may shift where input prices or policy support differ. Our estimates nevertheless show that the modeled frontier for durable removal can already reach \$29/tCO_2 under favorable conditions. This approaches the estimated marginal abatement cost of \$20–\$50/tCO_2 for non-permanent, reversible pathways such as tropical reforestation[105].

Across the four technologies, lower modeled costs generally coincide with more difficult MRV. DAC and BECCS can meter captured and injected CO_2, although they require input carbon accounting and leakage tracking. BiCRS adds biomass origin and permanence estimates, while ERW must infer uptake from dispersed field measurements and models against uncertain baselines. This distinction is becoming relevant beyond voluntary markets. Recently, the European Commission proposed integrating permanent removals into the European Union Emissions Trading System (EU ETS)[15]. The proposal states that one unit should represent one net ton after deducting life-cycle emissions. It further identifies permanence, reversal liability, MRV uncertainty, environmental effects, and technological maturity as conditions for ETS integration[16]. The assessment regards DAC and BECCS as ready for consideration, biochar as conditional, and enhanced weathering as requiring further research. ERW is also not currently eligible for U.S. tax credits.

Because durable carbon removal is a public good, the role of the state can extend beyond setting accounting rules[106]. This includes funding common MRV capabilities, demonstration projects, shared infrastructure, and early procurement through auctions or offtake agreements[107]. There is no need to transfer all project-performance risk to the state: payments can be tied to independently verified delivery, and contract design can incorporate non-delivery risk explicitly. Future work should quantify pathway-specific MRV costs, test how buyers value durability and delivery risk, and evaluate cost-efficient portfolios under common net-ton accounting.

Offtake agreements today apply inconsistent system boundaries, which invites boundary shopping. Contracts, registries, and support programs should therefore report gross sequestration, attributable emissions, net removal, co-product revenue, and public support. They should also disclose emission scope coverage, biogenic treatment, durability, verification rules, and excluded counterfactuals. These disclosures would enable more consistent quantification of net removal cost across technologies and projects. They further reveal when gross-based crediting schemes allocate more public support per net ton to configurations with higher leakage. Where public support targets atmospheric removal, payment should be tied to independently verified net tons to align incentives between project developers, buyers and governments. Scaling durable removal will require multiple technologies, but it should not require multiple definitions of a ton removed. LCCDR provides a common economic basis for comparing the cost of removing a net ton of CO_2.

Methods

Model Details

This section first verifies the formal Claim stated in the Economic Model and then provides a more detailed decomposition of the different LCCDR metrics. We recall from Economic Model that taxable income in year i is given by:

$$I_i(p,\vec{q}) = \sum_{t=1}^{m} [\, p \cdot (1-\alpha) \cdot q_{it} + CPR_{it}(q_{it}) - w_{it}(q_{it})] - f_i(k) - d_i \cdot v(k)$$

Further, the after-tax cash flows are given by:

$$DCF(p,\vec{q}) = DCF^o(p,\vec{q}) - \sum_{i=1}^{T} \tau \cdot I_i(p,\vec{q}) \cdot \gamma^i. \tag{4}$$

LCCDR is defined as the lowest value p at which the project breaks even:

$$DCF^*(p) = \max_{\vec{q}\in F} DCF(p,\vec{q}) \equiv DCF(p,\vec{q}^{\,*}(p)) = 0, \tag{5}$$

where

$$F = \{\vec{q} \mid q_{it} \leq k \text{ and} \sum_{i=1}^{T}\sum_{t=1}^{m} q_{it} \leq K\}$$

denotes the set of feasible utilization schedules. Assuming that $DCF^*(p = 0) < 0$, the linearity of $DCF(p,\vec{q})$ in p implies that $DCF^*(p) > 0$ for values of p sufficiently large. Assuming the component functions of $DCF(p,\vec{q})$ are continuous, the function $DCF(\cdot,\cdot)$ is continuous in both p and $\vec{q}$. The Berge Maximum Theorem then says that $DCF^*(\cdot)$ is continuous in p. By the Intermediate Value Theorem, there exists a value p^o such that $DCF^*(p^o) = 0$.

The uniqueness of p^o follows directly from the following "revealed preference" argument. Suppose that $p^2 > p^1$ and yet $DCF^*(p^2) = DCF^*(p^1) = 0$. That would yield the following contradiction:

$$0 = DCF^*(p^1) = DCF(p^1,\vec{q}^{\,*}(p^1)) < DCF(p^2,\vec{q}^{\,*}(p^1)) \leq DCF(p^2,\vec{q}^{\,*}(p^2)) = DCF^*(p^2) = 0.$$

Thus, the LCCDR is the unique value satisfying $DCF^*(LCCDR) = 0$. The expression for taxable income, $I_i(\cdot)$, allows us to *implicitly* solve the equation $DCF^*(\cdot) = 0$.

$$LCCDR = \frac{\sum_{i=1}^{T} [\sum_{t=1}^{m} [w_{it}(q_{it}^*(LCCDR)) - CPR_{it}(q_{it}^*(LCCDR))] + f_i(k)] \cdot \gamma^i + v(k) \cdot \Delta}{(1-\alpha) \cdot \sum_{i=1}^{T} \sum_{t=1}^{m} q_{it}^*(LCCDR) \cdot \gamma^i}. \tag{6}$$

Here Δ represents a mark-up factor given by:

$$\Delta = \frac{1 - \tau \cdot \sum_{i=1}^{T} d_i \cdot \gamma^i}{1-\tau}. \tag{7}$$

This mark-up is applied only to the original capital expenditure and summarizes the effects of income taxes via the applicable income tax rate, τ and the allowable depreciation schedule $(d_1, ...d_T)$. Clearly $\Delta \geq 1$, and $\Delta = 1$ absent any income taxes, that is $\tau = 0$. We note in passing that the preceding model formulation has implicitly assumed that co-product revenues constitute taxable income. For BECCS and DAC projects in the U.S., significant co-product revenues take the form of production tax credits which effectively amount to an after-tax revenue. If the co-product revenues take the form of production tax credits, equation (6) must be modified so that $CPR_{it}(q_{it}^*(LCCDR))$ is marked up by the factor $\frac{1}{1-\tau}$.

The representation of LCCDR in equation (6) conforms to the standard representation of the levelized cost of energy: total discounted cost over total discounted energy produced. In our context, this translates into: total discounted cost, less co-product revenues, over total discounted net tons of CO_2 removed.

Equation (6) is readily modified to characterize the levelized cost of CDR if one were to ignore any offsetting emissions, that is, α is set to zero. The corresponding lower levelized cost figure, $LCCDR^-$, is given as the unique solution to the equation:

$$LCCDR^- = \frac{\sum_{i=1}^{T} [\sum_{t=1}^{m} [w_{it}(q_{it}^*(LCCDR^-)) - CPR_{it}(q_{it}^*(LCCDR^-))] + f_i(k)] \cdot \gamma^i + v(k) \cdot \Delta}{\sum_{i=1}^{T} \sum_{t=1}^{m} q_{it}^*(LCCDR^-) \cdot \gamma^i}. \tag{8}$$

Economic Model defined $LCCDR^+$ as the levelized cost measure that obtains if the co-product revenues, $CPR(\cdot)$, are excluded from consideration, possibly because they vary considerably across locations. We then obtain:

$$LCCDR^{+} = \frac{\sum_{i=1}^{T} \left[\sum_{t=1}^{m} w_{it}(q_{it}^{*}(LCCDR^{+})) + f_i(k)\right] \cdot \gamma^i + v(k) \cdot \Delta}{(1-\alpha) \cdot \sum_{i=1}^{T} \sum_{t=1}^{m} q_{it}^{*}(LCCDR^{+}) \cdot \gamma^i}. \tag{9}$$

We note that the right-hand side of equation (6) yields an explicit solution for LCCDR if it is feasible and financially advantageous to use the achievable capacity throughout the modeled operating schedule, that is, $q_{it}^{*} = k$ in each available hour. We then obtain:

$$LCCDR = \frac{\sum_{i=1}^{T} \left[\sum_{t=1}^{m} \left[w_{it}(k) - CPR_{it}(k)\right] + f_i(k)\right] \cdot \gamma^i + v(k) \cdot \Delta}{(1-\alpha) \cdot m \cdot k \cdot \sum_{i=1}^{T} \gamma^i}. \tag{10}$$

Decomposing equation (10) yields the per-net components as defined directly before Table 1 in Results.

Model Calibration

For the reported configurations, annual operation is summarized by a constant capacity factor over the project lifetime. Full use of the nameplate capacity is generally not attainable in practice. The practical capacity k accounts for scheduled maintenance, anticipated downtime, and outages. BiCRS and BECCS operate at their technically achievable maxima, while DAC operates at or near its maintenance-constrained maximum because capacity cost dominates variable operating cost. The technology-specific capacity factors are approximately 84–90% and are reported in Supplementary Note 1.

We test the dispatch flexibility developed above for DAC by resolving utilization on an hourly grid-price vector. In the reported calibrations, however, the price-responsive margin never binds below the maintenance-constrained maximum. Capacity-related charges dominate the DAC cost structure. The break-even removal price is high relative to hourly variable cost, so the contribution margin of an additional operating hour remains positive even in expensive hours. It is thus optimal to keep the plant running even in hours with above-average power prices. The same applies to BECCS, where removal prices and tax credits are sufficient to justify continuous operation, even in hours with low electricity prices. Timing scheduled maintenance and downtime into the lowest-price hours can modestly raise co-product revenue without reducing annual output. These checks are reported in Supplementary Note 5. We note that price-responsive curtailment may become economically relevant for cost structures with a substantially higher variable-cost share.

The technology calculators first produce components per gross ton captured and sequestered, denoted c^g, f^g, w^g, and CPR^g. For any component x, its contribution per net ton is $x = x^g/(1-\alpha)$. The main text therefore reports all components consistently per net ton. The capacity-cost row in Table 1 includes the tax adjustment Δ, the variable-cost row includes transport and storage, and LCCDR$^-$ is calculated by setting $\alpha = 0$.

In the U.S. calibration the capacity costs are tax adjusted and include a depreciation tax shield. We apply a 21% federal corporate income-tax rate and, where applicable, a representative state tax rate. Depreciation is based on a seven-year Modified Accelerated Cost Recovery System (MACRS) depreciation schedule[108]. For DAC and BECCS, the 45Q credit is given as after-tax revenue paid per gross ton captured. It is therefore pre-tax adjusted by $1/(1-\tau)$, discounted over its 12-year statutory availability, and re-levelized over the applicable project lifetime.

Grid-electricity emissions use annual location-based intensities; renewable-coupled configurations use their modeled project supply mix (see Supplementary Note 1). The biomass main cases apply the biogenic-neutral convention, while Supplementary Note 4 reports the alternative boundary. BiCRS co-product revenue is the physical biochar sales price and is separate from the removal-credit price p. For ERW, the main case credits application-year uptake, $q_{it} = z_{it}\mu_0$. The timing sensitivity extends uptake using $\mu_j = \omega(1-\omega)^j Y^{\max}$ and discounts each verified future increment; see Supplementary Note 7.5.

The BiCRS equipment cost is based on a supplier quotation for a slow-pyrolysis unit, scaled to the 1 t/h reference size. For context, a survey of European pyrolysis suppliers reports a mean specific purchase price of 5,800 EUR per (kg/h) of feedstock capacity, a median of 6,600, and a biomass-only mean of 5,500, and quotes continuous units at 1.85 to 6.5 M EUR at 0.5 t/h and 3.4 M EUR at 1.0 t/h[109]. Our estimate corresponds to roughly 4,800 EUR per (kg/h) and therefore sits below that survey mean. The same survey finds no systematic relationship between specific purchase price and capacity over the 0.09 to 1.0 t/h range it covers. This is stress-tested in Supplementary Table 12.

The calibration sources and robustness checks are reported in the supplementary information. Technology-specific inputs, data sources, financial assumptions, and configuration changes are grouped in Supplementary Note 1. The calibration combines various source groups: peer-reviewed engineering and techno-economic studies; company estimates; government data on energy, emissions, taxation, and policy; registry methodologies; and disclosed transaction data. Excel workbooks provide technology-specific calibration anchors; Python implementations are available to reproduce quick configuration results and sensitivity checks. Because the underlying monetary sources use different price years and not every input can be restated consistently to a common base year, the results should be read as approximate current U.S. dollar costs. Complete configuration-level inputs and outputs and the reproducible model implementation are available as described in the Code availability statement.

Project Configurations

Comparisons between and within technologies are inherently difficult. We therefore define a set of plausible *project configurations* for each technology. Each specifies a complete set of techno-economic assumptions for a given case. A common one-at-a-time sensitivity analysis for all four technologies is reported in Supplementary Note 3. For the base cases, BECCS Wood is calibrated as a U.S. greenfield plant using woody residues. The supporting analysis tests plant and biomass costs, capture performance, utilization, and electricity revenue. Alternative treatments of biogenic carbon, upstream biomass emissions, and land-use change are reported in Supplementary Note 4. BiCRS is calibrated as a standard wood-based slow-pyrolysis plant in the U.S. Southeast. The supporting analysis tests plant and feedstock costs, feedstock emissions, utilization, and biochar revenue. Alternative biomass-accounting boundaries are reported in the same note as BECCS. The effect of restricting removal credits to the bio-oil stream is shown in Supplementary Note 4.4. DAC plants are calibrated as current commercial-grid plants for the two capture chemistries. The supporting analysis tests capital and operating costs, utilization, energy supply, and transport and storage. Policy support is examined in Supplementary Note 2. Future configurations are reported in Supplementary Note 6.1, and hourly utilization is examined in Supplementary Note 5. ERW Basalt and Dunite combine mostly mid-west U.S. cost, transport, electricity, and agronomic inputs with reference weathering rates based on pH-7, 25 °C. The supporting analysis tests cost, transport, yield, and financing assumptions. The clean-electricity diagnostic is reported in Supplementary Note 6.2. Regional deployment conditions, grain size, weathering rates, MRV cost, and removal timing are examined in Supplementary Note 7.

Below we detail the alternative project configurations and IDs in Table 2. For DAC we report three current project configurations in the main body: SD1/LD1 (Frontier, a first-of-a-kind plant), SD2/LD2 (Commercial-Grid, a base commercial plant using regional grid electricity), and SD3/LD3 (Renewable-Coupled, the same plant architecture as SD2/LD2 with co-invested Wind & Solar electricity and grid backup retained). The future-horizon SD4/LD4 (Mature-2030) and SD5/LD5 (Long-term-2050) cases are documented in Supplementary Table 16.

Technology	ID	Project configuration	α (%)	LCCDR^-	LCCDR ($/t$CO_2$)	LCCDR^+
S-DAC	SD1	Frontier	41.17	633	1076	1416
S-DAC	SD2	Commercial-Grid	34.16	324	492	796
S-DAC	SD3	Renewable-Coupled	25.26	318	426	694
L-DAC	LD1	Frontier	37.17	422	671	950
L-DAC	LD2	Commercial-Grid	32.61	195	290	549
L-DAC	LD3	Renewable-Coupled	24.17	186	245	476
BECCS	BE1	Greenfield-Wood	4.60	85	89	196
BECCS	BE2	Greenfield-CropResidue	6.97	102	109	218
BECCS	BE3	Greenfield-EnergyCrop	7.16	115	123	234
BiCRS	BC1	Favorable-Wood	4.91	93	98	129
BiCRS	BC2	Realistic-Wood	5.22	101	107	139
BiCRS	BC3	Conservative-Residue	11.21	145	163	221
ERW Basalt	EB1	Favorable	3.66	121	125	148
ERW Basalt	EB2	Realistic	32.28	176	260	280
ERW Basalt	EB3	Conservative	38.16	210	340	353
ERW Dunite	ED1	Favorable	0.90	29	29	29
ERW Dunite	ED2	Realistic	3.92	46	48	48
ERW Dunite	ED3	Conservative	6.62	66	70	70

Table 2. LCCDR summary for the current project configurations. This table shows the leakage factor α and the levelized removal cost under three system-boundary conventions: LCCDR^- ignores leakage ($\alpha = 0$), the main LCCDR includes leakage and is net of co-product revenues, and LCCDR^+ includes leakage but excludes co-product revenues (including the 45Q tax credit); by construction $\text{LCCDR}^- \leq \text{LCCDR} \leq \text{LCCDR}^+$. The policy-support (45Q) decomposition and the policy-free values for the eligible pathways are reported separately in Supplementary Note 2.

For BECCS we define three greenfield project configurations by feedstock type: BE1 (Wood; woody residues), BE2 (CropResidue; crop-residue or waste biomass with higher logistics effort), and BE3 (EnergyCrop; a dedicated miscanthus energy crop), each with upstream emissions built from a feedstock-specific feedstock-emissions term and a delivery-transport term. For BiCRS we define three project configurations by feedstock and transport: BC1 (Favorable-Wood), BC2 (Realistic-Wood), and BC3 (Conservative-Residue). The three configurations jointly vary feedstock type, feedstock price, and transport distance, with

Conservative-Residue using corn stover and the longest transportation distance. For ERW we define three project configurations per rock type: EB1 (Basalt-Favorable), EB2 (Basalt-Realistic), EB3 (Basalt-Conservative), ED1 (Dunite-Favorable), ED2 (Dunite-Realistic), and ED3 (Dunite-Conservative). The Conservative cases are moderate stress configurations. The models support evaluation of additional configurations. Complete configuration-level inputs and outputs are documented in Supplementary Note 1.

Code availability

The models, complete configuration inputs and outputs, source code, and user documentation are available from the authors upon reasonable request. A public replication repository will be released with the journal submission.

References

[1] Calvin, K. *et al.* IPCC, 2023: Climate Change 2023: Synthesis Report. Sixth Assessment Report of the Intergovernmental Panel on Climate Change. Tech. Rep., Intergovernmental Panel on Climate Change (IPCC) (2023).

[2] Smith, S. *et al.* The State of Carbon Dioxide Removal - 2nd Edition (2024).

[3] Hilaire, J. *et al.* Negative emissions and international climate goals—learning from and about mitigation scenarios. *Climatic Change* **157**, 189–219 (2019).

[4] Schleussner, C.-F. *et al.* Overconfidence in climate overshoot. *Nature* **634**, 366–373 (2024).

[5] Gidden, M. J. *et al.* Fairness and feasibility in deep mitigation pathways with novel carbon dioxide removal considering institutional capacity to mitigate. *Environmental Research Letters* **18**, 074006 (2023).

[6] Buck, H. J., Carton, W., Lund, J. F. & Markusson, N. Why residual emissions matter right now. *Nature Climate Change* **13**, 351–358 (2023).

[7] Lamb, W. F. *et al.* The carbon dioxide removal gap. *Nature Climate Change* **14**, 644–651 (2024).

[8] IEA. Net Zero Roadmap: A Global Pathway to Keep the 1.5 °C Goal in Reach – Analysis. Tech. Rep. (2023).

[9] Rinberg, A., Bergman, A. M., Schrag, D. P. & Aziz, M. J. Alkalinity Concentration Swing for Direct Air Capture of Carbon Dioxide. *ChemSusChem* **14**, 4439–4453 (2021).

[10] Prütz, R., Strefler, J., Rogelj, J. & Fuss, S. Understanding the carbon dioxide removal range in 1.5 °C compatible and high overshoot pathways. *Environmental Research Communications* **5**, 041005 (2023).

[11] Powis, C. M., Smith, S. M., Minx, J. C. & Gasser, T. Quantifying global carbon dioxide removal deployment. *Environmental Research Letters* **18**, 024022 (2023).

[12] Edwards, M. R. *et al.* The State of Carbon Dioxide Removal - 3rd Edition (2026). OSF (2026). URL `https://osf.io/zrd65/`.

[13] DoE. Carbon Negative Shot (2021).

[14] 117th United States Congress. H.R.5376 - inflation reduction act of 2022 (IRA): Public law no: 117-169 (2022).

[15] European Commission. Commission boosts europe's competitiveness, decarbonisation and independence with electrification action plan and ETS review (2026). URL `https://ec.europa.eu/commission/presscorner/detail/en/ip_26_1596`. Press release IP/26/1596, 17 July 2026.

[16] European Commission. Impact assessment accompanying the 2026 review of the EU emissions trading system, part 3/5. Tech. Rep. SWD(2026) 616 final, Directorate-General for Climate Action, Brussels (2026). URL `https://climate.ec.europa.eu/publications/swd2026-616-impact-assessment_en`.

[17] Young, J. *et al.* The cost of direct air capture and storage can be reduced via strategic deployment but is unlikely to fall below stated cost targets. *One Earth* **6**, 899–917 (2023).

[18] Fuss, S. *et al.* Negative emissions—Part 2: Costs, potentials and side effects. *Environmental Research Letters* **13**, 063002 (2018).

[19] CDR.fyi. https://www.cdr.fyi/ (2025).

[20] Terlouw, T., Bauer, C., Rosa, L. & Mazzotti, M. Life cycle assessment of carbon dioxide removal technologies: A critical review. *Energy & Environmental Science* **14**, 1701–1721 (2021).

[21] Terlouw, T., Treyer, K., Bauer, C. & Mazzotti, M. Life Cycle Assessment of Direct Air Carbon Capture and Storage with Low-Carbon Energy Sources. *Environmental Science & Technology* **55**, 11397–11411 (2021).

[22] Sievert, K., Schmidt, T. S. & Steffen, B. Considering technology characteristics to project future costs of direct air capture. *Joule* **8**, 979–999 (2024).

[23] Titus, K., Dempsey, D., Peer, R. & Archer, R. Carbon Negative Geothermal: Techno-Economic Analysis of Geothermal Energy combined with Direct and Biomass-Based Carbon Dioxide Removal (2023).

[24] Mazzotti, M., Baciocchi, R., Desmond, M. J. & Socolow, R. H. Direct air capture of CO2 with chemicals: Optimization of a two-loop hydroxide carbonate system using a countercurrent air-liquid contactor. *Climatic Change* **118**, 119–135 (2013).

[25] Zeman, F. Reducing the Cost of Ca-Based Direct Air Capture of CO_2. *Environmental Science & Technology* **48**, 11730–11735 (2014).

[26] Keith, D. W., Holmes, G., St. Angelo, D. & Heidel, K. A process for capturing CO2 from the atmosphere. *Joule* 1–22 (2018).

[27] Kulkarni, A. R. & Sholl, D. S. Analysis of Equilibrium-Based TSA Processes for Direct Capture of CO_2 from Air. *Industrial & Engineering Chemistry Research* **51**, 8631–8645 (2012).

[28] Stolaroff, J. K., Keith, D. W. & Lowry, G. V. Carbon Dioxide Capture from Atmospheric Air Using Sodium Hydroxide Spray. *Environmental Science & Technology* **42**, 2728–2735 (2008).

[29] Lackner, K. S. & Azarabadi, H. Buying down the Cost of Direct Air Capture. *Industrial & Engineering Chemistry Research* **60**, 8196–8208 (2021).

[30] Daniel, T. *et al.* Techno-economic Analysis of Direct Air Carbon Capture with CO2 Utilisation. *Carbon Capture Science & Technology* **2**, 100025 (2022).

[31] Slavin, B., Wang, R., Roy, D., Ling-Chin, J. & Roskilly, A. P. Techno-economic analysis of direct air carbon capture and hydrogen production integrated with a small modular reactor. *Applied Energy* **356**, 122407 (2024).

[32] Lux, B., Schneck, N., Pfluger, B., Männer, W. & Sensfuß, F. Potentials of direct air capture and storage in a greenhouse gas-neutral European energy system. *Energy Strategy Reviews* **45**, 101012 (2023).

[33] Sabatino, F., Gazzani, M., Gallucci, F. & Van Sint Annaland, M. Modeling, Optimization, and Techno-Economic Analysis of Bipolar Membrane Electrodialysis for Direct Air Capture Processes. *Industrial & Engineering Chemistry Research* **61**, 12668–12679 (2022).

[34] Gutsch, M. & Leker, J. Co-assessment of costs and environmental impacts for off-grid direct air carbon capture and storage systems. *Communications Engineering* **3**, 14 (2024).

[35] Prats-Salvado, E., Jagtap, N., Monnerie, N. & Sattler, C. Solar-Powered Direct Air Capture: Techno-Economic and Environmental Assessment. *Environmental Science & Technology* **58**, 2282–2292 (2024).

[36] McQueen, N. *et al.* Cost Analysis of Direct Air Capture and Sequestration Coupled to Low-Carbon Thermal Energy in the United States. *Environmental Science & Technology* **54**, 7542–7551 (2020).

[37] Sinha, A., Darunte, L. A., Jones, C. W., Realff, M. J. & Kawajiri, Y. Systems Design and Economic Analysis of Direct Air Capture of CO_2 through Temperature Vacuum Swing Adsorption Using MIL-101(Cr)-PEI-800 and mmen-Mg_2 (dobpdc) MOF Adsorbents. *Industrial & Engineering Chemistry Research* **56**, 750–764 (2017).

[38] Bossio, D. A. *et al.* The role of soil carbon in natural climate solutions. *Nature Sustainability* **3**, 391–398 (2020).

[39] Roe, S. *et al.* Land-based measures to mitigate climate change: Potential and feasibility by country. *Global Change Biology* **27**, 6025–6058 (2021).

[40] Yablonovitch, E. & Deckman, H. W. Scalable, economical, and stable sequestration of agricultural fixed carbon. *Proceedings of the National Academy of Sciences* **120**, e2217695120 (2023).

[41] Langholtz, M. *et al.* The Economic Accessibility of CO2 Sequestration through Bioenergy with Carbon Capture and Storage (BECCS) in the US. *Land* **9**, 299 (2020).

[42] Lozano, E., Petersen, S., Paulsen, M., Rosendahl, L. & Pedersen, T. Techno-economic evaluation of carbon capture via physical absorption from HTL gas phase derived from woody biomass and sewage sludge. *Energy Conversion and Management: X* **11**, 100089 (2021).

[43] Lim, T. C., Cuellar, A., Langseth, K. & Waldon, J. L. Technoeconomic Analysis of Negative Emissions Bioenergy with Carbon Capture and Storage through Pyrolysis and Bioenergy District Heating Infrastructure. *Environmental Science & Technology* **56**, 1875–1884 (2022).

[44] Emenike, O., Michailos, S., Hughes, K. J., Ingham, D. & Pourkashanian, M. Techno-economic and environmental assessment of BECCS in fuel generation for FT-fuel, bioSNG and OME x. *Sustainable Energy & Fuels* **5**, 3382–3402 (2021).

[45] Beiron, J., Normann, F. & Johnsson, F. A techno-economic assessment of CO2 capture in biomass and waste-fired combined heat and power plants – A Swedish case study. *International Journal of Greenhouse Gas Control* **118**, 103684 (2022).

[46] Pratama, M. R., Muthia, R. & Purwanto, W. W. Techno-economic and life cycle assessment of the integration of bioenergy with carbon capture and storage in the polygeneration system (BECCS-PS) for producing green electricity and methanol. *Carbon Neutrality* **2**, 26 (2023).

[47] Restrepo-Valencia, S. & Walter, A. Techno-Economic Assessment of Bio-Energy with Carbon Capture and Storage Systems in a Typical Sugarcane Mill in Brazil. *Energies* **12**, 1129 (2019).

[48] Wu, N., Lan, K. & Yao, Y. An integrated techno-economic and environmental assessment for carbon capture in hydrogen production by biomass gasification. *Resources, Conservation and Recycling* **188**, 106693 (2023).

[49] Beerling, D. J. *et al.* Farming with crops and rocks to address global climate, food and soil security. *Nature Plants* **4**, 138–147 (2018).

[50] Beerling, D. J. *et al.* Enhanced weathering in the US Corn Belt delivers carbon removal with agronomic benefits. *Proceedings of the National Academy of Sciences* **121**, e2319436121 (2024).

[51] Beerling, D. J. *et al.* Transforming US agriculture for carbon removal with enhanced weathering. *Nature* **638**, 425–434 (2025).

[52] Goll, D. S. *et al.* Potential CO2 removal from enhanced weathering by ecosystem responses to powdered rock. *Nature Geoscience* **14**, 545–549 (2021).

[53] Chambers, A., Lal, R. & Paustian, K. Soil carbon sequestration potential of US croplands and grasslands: Implementing the 4 per Thousand Initiative. *Journal of Soil and Water Conservation* **71**, 68A–74A (2016).

[54] Kelemen, P., Benson, S. M., Pilorgé, H., Psarras, P. & Wilcox, J. An Overview of the Status and Challenges of CO2 Storage in Minerals and Geological Formations. *Frontiers in Climate* **1**, 9 (2019).

[55] Strefler, J., Amann, T., Bauer, N., Kriegler, E. & Hartmann, J. Potential and costs of carbon dioxide removal by enhanced weathering of rocks. *Environmental Research Letters* **13**, 034010 (2018).

[56] Zhang, B., Kroeger, J., Planavsky, N. & Yao, Y. Techno-Economic and Life Cycle Assessment of Enhanced Rock Weathering: A Case Study from the Midwestern United States. *Environmental Science & Technology* **57**, 13828–13837 (2023).

[57] Jiang, H., Wang, S., Xing, L., Pinfield, V. J. & Xuan, J. Machine learning based techno-economic process optimisation for CO2 capture via enhanced weathering. *Energy and AI* **12**, 100234 (2023).

[58] Cobo, S. *et al.* Sustainable scale-up of negative emissions technologies and practices: Where to focus. *Environmental Research Letters* **18**, 023001 (2023).

[59] Chiquier, S., Gurgel, A., Morris, J., Chen, Y.-H. H. & Paltsev, S. Integrated assessment of carbon dioxide removal portfolios: Land, energy, and economic trade-offs for climate policy. *Environmental Research Letters* **20**, 024002 (2025).

[60] Hickey, C., Jenkins, S. & Allen, M. Carbon storage portfolios for the transition to net zero. *Joule* **0** (2025).

[61] Mühlbauer, A. *et al.* Assessment of technologies and economics for carbon dioxide removal from a portfolio perspective. *International Journal of Greenhouse Gas Control* **141**, 104297 (2025).

[62] NASEM *et al.* *Negative Emissions Technologies and Reliable Sequestration: A Research Agenda* (National Academies Press, Washington, D.C., 2019).

[63] Pett-Ridge, J. *et al.* Roads to Removal: Options for Carbon Dioxide Removal in the United States. Tech. Rep. LLNL–TR-852901, 2301853, 1080440 (2023).

[64] Nordahl, S. L. *et al.* Carbon accounting for carbon dioxide removal. *One Earth* **7**, 1494–1500 (2024).

[65] MIT. The future of coal: Options for a carbon-constrained world (2007).

[66] Comello, S. D., Glenk, G. & Reichelstein, S. Levelized cost of electricity calculator (2017).

[67] Glenk, G., Holler, P. & Reichelstein, S. Advances in power-to-gas technologies: Cost and conversion efficiency. *Energy & Environmental Science* **16**, 6058–6070 (2023).

[68] Weimann, G. G. & Bentsen, N. S. Potential for carbon dioxide removal of carbon capture and storage on biomass-fired combined heat and power production. *GCB Bioenergy* **16**, e13184 (2024).

[69] Brandl, P., Bui, M., Hallett, J. P. & Mac Dowell, N. Beyond 90% capture: Possible, but at what cost? *International Journal of Greenhouse Gas Control* **105**, 103239 (2021).

[70] Lehtveer, M. & Emanuelsson, A. BECCS and DACCS as Negative Emission Providers in an Intermittent Electricity System: Why Levelized Cost of Carbon May Be a Misleading Measure for Policy Decisions. *Frontiers in Climate* **3**, 647276 (2021).

[71] Mac Dowell, N., Reiner, D. M. & Haszeldine, R. S. Comparing approaches for carbon dioxide removal. *Joule* **6**, 2233–2239 (2022).

[72] Prado, A. & Mac Dowell, N. The cost of permanent carbon dioxide removal. *Joule* **7**, 700–712 (2023).

[73] Cheng, F., Small, A. A. & Colosi, L. M. The levelized cost of negative CO2 emissions from thermochemical conversion of biomass coupled with carbon capture and storage. *Energy Conversion and Management* **237**, 114115 (2021).

[74] ERM. A Review of Engineered Greenhouse Gas Removal (GGR) Standards and Methodologies. Tech. Rep. (2023).

[75] EBI. Biochar-based carbon sinks to mitigate climate change. Tech. Rep. (2020).

[76] Kung, C.-C., McCarl, B. A. & Cao, X. Economics of pyrolysis-based energy production and biochar utilization: A case study in Taiwan. *Energy Policy* **60**, 317–323 (2013).

[77] Tripathi, M., Sahu, J. & Ganesan, P. Effect of process parameters on production of biochar from biomass waste through pyrolysis: A review. *Renewable and Sustainable Energy Reviews* **55**, 467–481 (2016).

[78] Campbell, R. M., Anderson, N. M., Daugaard, D. E. & Naughton, H. T. Financial viability of biofuel and biochar production from forest biomass in the face of market price volatility and uncertainty. *Applied Energy* **230**, 330–343 (2018).

[79] Racek, J., Sevcik, J., Chorazy, T., Kucerik, J. & Hlavinek, P. Biochar – Recovery Material from Pyrolysis of Sewage Sludge: A Review. *Waste and Biomass Valorization* **11**, 3677–3709 (2020).

[80] Stallkamp, C., Hennig, M., Volk, R., Stapf, D. & Schultmann, F. Pyrolysis of mixed engineering plastics: Economic challenges for automotive plastic waste. *Waste Management* **176**, 105–116 (2024).

[81] Dhyani, V. & Bhaskar, T. A comprehensive review on the pyrolysis of lignocellulosic biomass. *Renewable Energy* **129**, 695–716 (2018).

[82] Amenaghawon, A. N., Anyalewechi, C. L., Okieimen, C. O. & Kusuma, H. S. Biomass pyrolysis technologies for value-added products: A state-of-the-art review. *Environment, Development and Sustainability* **23**, 14324–14378 (2021).

[83] Tomczyk, A., Sokołowska, Z. & Boguta, P. Biochar physicochemical properties: Pyrolysis temperature and feedstock kind effects. *Reviews in Environmental Science and Bio/Technology* **19**, 191–215 (2020).

[84] Azzi, E. S., Li, H., Cederlund, H., Karltun, E. & Sundberg, C. Modelling biochar long-term carbon storage in soil with harmonized analysis of decomposition data. *Geoderma* **441**, 116761 (2024).

[85] Lehmann, J. *et al.* Biochar in climate change mitigation. *Nature Geoscience* **14**, 883–892 (2021).

[86] Frank, J. R., Brown, T. R., Malmsheimer, R. W., Volk, T. A. & Ha, H. The financial trade-off between the production of biochar and biofuel via pyrolysis under uncertainty. *Biofuels, Bioproducts and Biorefining* **14**, 594–604 (2020).

[87] Schmidt, H.-P. *et al.* Biochar in agriculture – A systematic review of 26 global meta-analyses. *GCB Bioenergy* **13**, 1708–1730 (2021).

[88] You, F., Tao, L., Graziano, D. J. & Snyder, S. W. Optimal design of sustainable cellulosic biofuel supply chains: Multiobjective optimization coupled with life cycle assessment and input–output analysis. *AIChE Journal* **58**, 1157–1180 (2012).

[89] Strzalka, R., Schneider, D. & Eicker, U. Current status of bioenergy technologies in Germany. *Renewable and Sustainable Energy Reviews* **72**, 801–820 (2017).

[90] IEA. Direct Air Capture: A Key Technology for Net Zero. https://www.iea.org/energy-system/carbon-capture-utilisation-and-storage/direct-air-capture (2022).

[91] Deutz, S. & Bardow, A. Life-cycle assessment of an industrial direct air capture process based on temperature–vacuum swing adsorption. *Nature Energy* **6**, 203–213 (2021).

[92] Herzog, H., Morris, J., Gurgel, A. & Paltsev, S. Getting real about capturing carbon from the air. *One Earth* **7**, 1477–1480 (2024).

[93] Van Der Spek, M. *et al.* An ecosystem of carbon dioxide removal reviews – part 1: Direct air CO_2 capture and storage. *Energy & Environmental Science* **18**, 9713–9785 (2025).

[94] Erans, M. *et al.* Direct air capture: Process technology, techno-economic and socio-political challenges. *Energy & Environmental Science* **15**, 1360–1405 (2022).

[95] Madhu, K., Pauliuk, S., Dhathri, S. & Creutzig, F. Understanding environmental trade-offs and resource demand of direct air capture technologies through comparative life-cycle assessment. *Nature Energy* **6**, 1035–1044 (2021).

[96] Beerling, D. J. *et al.* Potential for large-scale CO2 removal via enhanced rock weathering with croplands. *Nature* **583**, 242–248 (2020).

[97] Campbell, J. S. *et al.* Geochemical Negative Emissions Technologies: Part I. Review. *Frontiers in Climate* **4** (2022).

[98] Bijma, J. *et al.* Reviews and syntheses: Carbon vs. cation based MRV of Enhanced Rock Weathering and the issue of soil organic carbon. *Biogeosciences* **23**, 53–75 (2026).

[99] Schiedung, M. *et al.* Uncertainties of enhanced rock weathering for climate-change mitigation. *Nature Reviews Earth & Environment* (2026).

[100] Beerling, D. J. *et al.* Challenges and opportunities in scaling enhanced weathering for carbon dioxide removal. *Nature Reviews Earth & Environment* **6**, 672–686 (2025).

[101] Isometric. Enhanced weathering in agriculture protocol, version 1.2. https://registry.isometric.com/protocol/enhanced-weathering-agriculture/1.2 (2026). Accessed 2026-07-28.

[102] Puro.earth. Enhanced rock weathering methodology, edition 2025 v.2. https://puro.earth/methodologies/enhanced-rock-weathering/ (2026). Approved 2026-03-05. Accessed 2026-07-28.

[103] Isometric. Isometric's verification fees. https://isometric.com/pricing (2026). Accessed 2026-06-11.

[104] Puro.earth. Puro.earth fee structure. https://puro.earth/certified-carbon-credits/fees/ (2026). Accessed 2026-06-11.

[105] Busch, J. *et al.* Potential for low-cost carbon dioxide removal through tropical reforestation. *Nature Climate Change* **9**, 463–466 (2019).

[106] Honegger, M., Poralla, M., Michaelowa, A. & Ahonen, H.-M. Who is paying for carbon dioxide removal? designing policy instruments for mobilizing negative emissions technologies. *Frontiers in Climate* **3**, 672996 (2021).

[107] European Scientific Advisory Board on Climate Change. Scaling up carbon dioxide removals: Recommendations for navigating opportunities and risks in the EU. Tech. Rep., European Scientific Advisory Board on Climate Change, Copenhagen (2025). URL `https://climate-advisory-board.europa.eu/`.

[108] U.S. IRS. Publication 946 (2019), how to depreciate property (2019).

[109] Klauser, F. *et al.* Pyrolysetechnologien in Europa: Technologieübersicht mittelschneller Pyrolyse für dezentrale Anwendungen, für kleine und mittlere Unternehmen und für die Kreislaufwirtschaft. Berichte aus Energie- und Umweltforschung 14/2024, BEST – Bioenergy and Sustainable Technologies GmbH, Wien (2024). URL `https://nachhaltigwirtschaften.at/resources/nw_pdf/schriftenreihe/schriftenreihe-2024-24-pyrolysetechnologien-europa.pdf`. Im Auftrag des Bundesministeriums für Klimaschutz, Umwelt, Energie, Mobilität, Innovation und Technologie (BMK). No DOI; no ISBN.

[110] U.S. Energy Information Administration. Monthly densified biomass fuel report. Form EIA-63C, U.S. Department of Energy (2024). URL `https://www.eia.gov/biofuels/biomass/archive/2024/03/csv/EIA_63C_Table_3.csv`. Table 3, Feedstocks and average cost per ton for the manufacture of densified biomass products; data through March 2024; costs reported per short ton; OMB No. 1905-0209.

[111] Rincione, R., Longo, S., Cellura, M., Guarino, F. & Brunetti, A. Life Cycle Assessment of Wood Chips from Residual Biomass: A Case Study. *International Journal of Sustainable Development and Planning* **18**, 2253–2258 (2023). URL `https://www.iieta.org/download/file/fid/103791`.

[112] U.S. Environmental Protection Agency. Emission factors for greenhouse gas inventories. GHG Emission Factors Hub, U.S. Environmental Protection Agency, Center for Corporate Climate Leadership (2025). URL `https://www.epa.gov/climateleadership/ghg-emission-factors-hub`. 2025 edition. Table 8, Scope 3 Categories 4 and 9, Medium- and Heavy-Duty Truck: 0.186 kg CO2, 0.0016 g CH4 and 0.0054 g N2O per short ton-mile.

[113] EIA. Opendata - U.S. Energy Information Administration (EIA). https://www.eia.gov/opendata/ (2024).

[114] Ember. Yearly Electricity Data. https://ember-energy.org/data/yearly-electricity-data/ (2024). Grid carbon-intensity series used for the U.S. average.

[115] IEAGHG. Global Assessment of Direct Air Capture Costs. Technical Report (2021).

[116] Lask, J. *et al.* A parsimonious model for calculating the greenhouse gas emissions of miscanthus cultivation using current commercial practice in the United Kingdom. *GCB Bioenergy* **13**, 1087–1098 (2021).

[117] Rubin, E. S. *et al.* A proposed methodology for CO2 capture and storage cost estimates. *International Journal of Greenhouse Gas Control* **17**, 488–503 (2013).

[118] Gustafsson, K., Sadegh-Vaziri, R., Grönkvist, S., Levihn, F. & Sundberg, C. BECCS with combined heat and power: Assessing the energy penalty. *International Journal of Greenhouse Gas Control* **108**, 103248 (2021).

[119] Smith, E. *et al.* The cost of CO2 transport and storage in global integrated assessment modeling. *International Journal of Greenhouse Gas Control* **109**, 103367 (2021).

[120] Hitachi Energy. Velocity suite - market intelligence services (2024).

[121] Skov, K. *et al.* Initial agronomic benefits of enhanced weathering using basalt: A study of spring oat in a temperate climate. *PLOS ONE* **19**, e0295031 (2024).

[122] U.S. Department of Agriculture, National Agricultural Statistics Service. Iowa Ag News – Crop Production. Tech. Rep., USDA National Agricultural Statistics Service, Upper Midwest Regional Field Office, Des Moines, IA (2025). URL `https://www.nass.usda.gov/Statistics_by_State/Iowa/Publications/Crop_Report/2025/IA-Crop-Production-Annual-01-25.pdf`. Crop Production 2024 Summary, Iowa release, 10 January 2025.

[123] Plevin, R. J., O'Hare, M., Jones, A. D., Torn, M. S. & Gibbs, H. K. Greenhouse gas emissions from biofuels' indirect land use change are uncertain but may be much greater than previously estimated. *Environmental Science & Technology* **44**, 8015–8021 (2010).

[124] Searchinger, T. *et al.* Use of U.S. croplands for biofuels increases greenhouse gases through emissions from land-use change. *Science* **319**, 1238–1240 (2008).

[125] Fargione, J., Hill, J., Tilman, D., Polasky, S. & Hawthorne, P. Land clearing and the biofuel carbon debt. *Science* **319**, 1235–1238 (2008).

[126] National Centers for Environmental Information. Summary of monthly normals, 1991–2020: Miami international airport, florida (2026). URL `https://www.ncei.noaa.gov/access/services/data/v1?dataset=normals-monthly-1991-2020&endDate=9996-12-31&format=pdf&startDate=0001-01-01&stations=USW00012839`. Station USW00012839; accessed 3 August 2026.

[127] Cipolla, G., Calabrese, S., Porporato, A. & Noto, L. V. Effects of precipitation seasonality, irrigation, vegetation cycle and soil type on enhanced weathering: Modeling of cropland case studies across four sites. *Biogeosciences* **19**, 3877–3896 (2022).

[128] Isometric. Isometric standard, version 2.1. https://registry.isometric.com/standard (2026). Accessed 2026-07-28.

Supplementary Information

Cost Comparisons for Emerging Carbon Dioxide Removal Technologies

Philip Holler
MISES, University of Mannheim
philip.holler@uni-mannheim.de

Stefan Reichelstein
MISES, University of Mannheim
Graduate School of Business, Stanford University
ZEW – Leibniz Centre for European Economic Research
reichelstein@uni-mannheim.de

August 2026

1 Data and Assumptions

This section consolidates data provenance and parameter assumptions. It shows how specific LCCDR values are derived: for each technology a *base-case* table lists the input values, the geographic source where applicable (U.S. Texas for DAC, U.S. Iowa for ERW, U.S. Georgia for BiCRS, EIA national defaults elsewhere), and the citation or model-calibration reference. Each base table is immediately followed by a companion table giving the variations per project configuration across that technology's full deployment set. Financial parameters (WACC, tax rates, depreciation schedules) are technology-specific and discussed at the end of the section. All monetary values are reported in U.S. dollars. Input prices are drawn from sources with different price years and cannot always be restated to a common base year. Whenever possible, inputs are escalated to the respective model base year using standard U.S. price indices. Reported costs should therefore be read as approximate current U.S. dollar costs. See details in the online supplementary information.

Parameter	Value	Unit	Geo.	Source
WACC	7	%	US	Literature/assumption
Plant lifetime	20	yr		
Capacity factor	90	%		Assumption
Equipment cost (1 t/h)	5.20	M$	US	Model Calibration;[109]
Feedstock price	36	\$/t BM	US	EIA [110]
Biomass harvest EF	23.7	kg CO_2/t BM	US	Rincione et al.[111]
Truck emission factor	0.128	kg CO_2e/t km	US	EPA GHG Emission Factors[112]
Biochar yield (dry)	0.35	t BC/t dry BM		[83]
Bio-oil yield (dry)	0.30	t BO/t dry BM		[83]
Biochar C content	0.80	kg C/kg BC		[85]
Permanence factor F_{p100}	0.80			[84;85]
Electricity price	0.0658	\$/kWh	US/GA	EIA [113]
Grid carbon intensity	0.369	kg CO_2e/kWh	US	Ember [114]
Biochar sale price	100	\$/t BC	US	Market-price assumption
T&S cost (biochar+bio-oil)	25.9	\$/t CO_2	US	[115]

Supplementary Table 1. BiCRS input assumptions. Base-case (BC2) parameter values, units, geography, and sources.

The BiCRS base case is the BC2 Realistic-Wood configuration (woodchips, Georgia); the three project configurations vary feedstock and transport distance, with BC3 substituting the feedstock to corn-stover residue at extended haul. The feedstock price is taken from the Q1 2024 U.S. national average delivered cost of sawmill residuals, used here as a Georgia proxy. As the underlying series is reported per short ton, we convert the \$36/t BM to \$39 per metric tonne. The harvest emissions cover extraction, chipping, collection with transport added separately using the respective truck emission factor and the configuration-specific distance. BC3 substitutes the biomass feedstock with corn stover (see details in the table below and in the online supplementary information).

Project configuration	Feedstock	Transport (km)	Feedstock price (\$/t BM)	Plant config
BC1 Favorable-Wood	Woodchips	25	27	Georgia
BC2 Realistic-Wood	Woodchips	50	36	Georgia
BC3 Conservative-Residue	Corn Stover	100	64	Iowa

Supplementary Table 2. BiCRS project configurations. Feedstock, transport distance, ex-mill feedstock price (transport modeled separately), and plant configuration across the three BiCRS project configurations.

The BECCS base case is BE1 Greenfield-Wood. The three greenfield project configurations span forest residue (BE1), crop-residues i.e. wheat straw (BE2), and a dedicated miscanthus energy crop (BE3). Within the main-case boundary BE2 and BE3 are close in terms of leakage, 7.0% against 7.2%. They separate materially only once a counterfactual land-use debit is added (see Supplementary Note 4.3). The BE3 feedstock-emissions factor of 57.7 $kgCO_2e/dry\,t$ is derived from Lask et al.[116]. The utilization factor in the BECCS case is based on an achievable, levelized capacity factor. It is the discount-weighted average, over the 25-year project life. For the 250 MW plant, we assume a staggered ramp-up from 40% and 65% in the first two operating years to 90% nameplate availability thereafter, which yields 84.1%. BiCRS plants are assumed to reach their 90% availability directly, as they are much smaller, modular plants.

In Supplementary Table 4, wheat straw serves as a generic crop-residue feedstock. It combines a sourced upstream emission factor for the biomass with configuration-specific assumed distances (see online tools). The distances are 100 km for BE1 and 150 km for BE2 and BE3, and 25, 50 and 100 km for BC1, BC2 and BC3, which results in extra upstream transport emissions of 12.8 $kgCO_2e/dry\,t$ for BE1 and 19.2 for BE2 and BE3. These distances are configuration assumptions. We take the emission factor of 0.128 $kgCO_2e/t\,km$, converted

Parameter	Value	Unit	Geo.	Source
WACC	7	%	US	Assumption
Plant lifetime	25	yr		[42]
Capacity factor (levelized)	84	%		Model-derived; levelization follows Rubin et al.[117]
Capture efficiency	90	%		Design parameter
Biomass price (delivered)	75	\$/dry t	US	Market-price assumption
Biomass carbon fraction	0.476	kg C/kg		Workbook calibration
Biomass higher heating value (HHV)	19.50	GJ/t		Workbook calibration
Upstream emissions	28.0 + 12.8	kgCO_2e/dry t	US	Feedstock emissions plus transport emissions; see Supplementary Table 4
Monoethanolamine (MEA) consumption	1.5	kg/t CO_2		[118]
Downstream T&S cost	20.9	\$/t CO_2	US	[115;119]
45Q credit (sequestration)	85	\$/t CO_2	US	IRA 2022[14]
Electricity revenue	44	\$/MWh	US	EIA [113]

Supplementary Table 3. BECCS input assumptions. Base-case (BE1) parameter values, units, geography, and sources.

from the U.S. Environmental Protection Agency's greenhouse gas emission factors hub from 2025 for medium- and heavy-duty trucks. The same factor is applied to both biomass technologies for comparability. This factor is tank-to-wheel, covering fuel combustion only, excluding the upstream production of that fuel. Including further emissions would not impact LCCDR much. A 10 kgCO_2e/dry t difference moves LCCDR by less than \$1/tCO_2.

The main analysis does not add counterfactual soil-carbon or avoided-decomposition credits. One qualification applies to the crop-residue configuration. Cultivation emissions of the parent cereal crop are allocated to the grain, so the straw carries only the consequences of its removal: nutrient replacement, meaning manufacture of the nitrogen, phosphate and potash physically exported with the straw, and the marginal field N_2O, meaning the N_2O from the replacement nitrogen net of the N_2O the residue nitrogen would itself have produced had it remained in the field. Charging the replacement nitrogen gross instead would raise BE2 upstream emissions from 72.2 to about 106 kgCO_2e/dry t, α from 7.0 to 9.3%, and LCCDR from \$109 to about \$112/tCO_2. Counterfactual soil organic carbon and indirect land-use change remain outside the main case for every configuration. Supplementary

Project configuration	Biomass type	Biomass price ($/dry t, delivered)	Upstream emissions ($kgCO_2e$/ dry t)	Carbon content	HHV (GJ/t)
BE1 Greenfield-Wood	Wood chips	75.0	28.0 + 12.8	0.476	19.50
BE2 Greenfield-CropResidue	Wheat straw	95.0	53.0 + 19.2	0.440	17.82
BE3 Greenfield-EnergyCrop	Miscanthus	110.0	57.7 + 19.2	0.452	19.16

Supplementary Table 4. BECCS project configurations. Biomass type, delivered price, upstream emissions, and feedstock properties across the three greenfield project configurations. Upstream emissions are reported as a feedstock-emissions term plus a transport term. The transport term is the one-way haul distance (100 km for BE1, 150 km for BE2 and BE3) times a single truck emission factor of 0.128 $kgCO_2e/t\,km$, taken from the U.S. EPA GHG Emission Factors Hub[112], Table 8, medium- and heavy-duty truck. No moisture or wet-to-dry adjustment is applied. The factor is tank-to-wheel, so it covers combustion only and excludes upstream fuel production.

Note 4.3 elaborates on land-use change dynamics.

The DAC base case is SD2/LD2 Commercial-Grid at 1 Mt CO_2/yr, and each project configuration is run for both chemistries (S-DAC solid sorbent, L-DAC liquid solvent). Across the current set, the configurations vary plant scale, capital-cost assumptions, and electricity supply. SD1/LD1 represent smaller Frontier plants run on the workbook's upper current-cost and conservative-performance case, which raises capital, fixed, variable, and transport-and-storage costs together with attributable emissions. SD3/LD3 isolate the effect of renewable coupling relative to SD2/LD2 by holding scale and plant architecture fixed. Location, cost of capital, and capacity factor remain constant. The Mature-2030 (SD4/LD4) and long-term 2050 (SD5/LD5) future-horizon project configurations, their input settings, and cost build-ups are reported in Supplementary Note 6.1.

The ERW base cases are EB2 Basalt-Realistic and ED2 Dunite-Realistic using Iowa cost, grid, logistics, and agronomic inputs together with pH 7, 25 °C reference weathering rates. The six project configurations vary rock type, grain size, application rate, and transport distance across Favorable, Realistic, and Conservative settings. Dunite has no agronomic co-product revenue. The Conservative configurations, EB3 and ED3, combine a coarser grind, a lower application rate, and a longer transport distance. EB3 also assumes lower agronomic co-product revenue.

The basalt co-product revenue reflects agronomic yield benefits from soil amendment.

Parameter	SD2 / LD2	Unit	Geo.	Source
WACC	10	%	US	Literature/assumption
Plant lifetime	15 / 20	yr		
Available capacity factor	85 / 85	%		Model Calibration
Initial capital cost (1 Mt/yr plant)	1,270 / 1,349	M$	US	[17;22]
Electricity consumption	0.475 / 0.450	MWh/t CO_2		[26;62]
Thermal energy	6.0 / 6.8	GJ/t CO_2		[26]
Electricity price	0.0768	$/kWh	US/TX	Velocity Suite[120], plus delivery adder (assumption)
Natural gas price	4.19	$/GJ	US/TX	EIA [113]
Grid carbon intensity	0.369	kg CO_2e/kWh	US/TX	Ember [114]
T&S cost	20.9	$/t CO_2	US	[115;119]
45Q credit (DAC, seq.)	180	$/t CO_2	US	IRA 2022[14]

Supplementary Table 5. DAC input assumptions. Base-case (SD2/LD2) parameter values for both chemistries, with units, geography, and sources. Paired values are ordered S-DAC / L-DAC.

Parameter	SD1/LD1	SD2/LD2	SD3/LD3
Forecast Horizon	Current	Current	Current
Techno-economic case	upper	base	base
Process energy inputs	Electricity + thermal	Electricity + thermal	Electricity + thermal
Electricity source	Grid	Grid	Wind & Solar
Thermal source	Natural Gas	Natural Gas	Natural Gas
Grid Connection	Yes	Yes	Yes
Nameplate Capacity (Mt/yr)	0.1	1.0	1.0

Supplementary Table 6. DAC project configurations. Forecast horizon, energy supply, and capacity settings across the three current DAC project configurations. The upper bound case jointly applies the workbook's upper cost and conservative performance assumptions, which raise capital, fixed, variable, and transport-and-storage costs as well as attributable emissions. The future-horizon project configurations (Mature-2030 SD4/LD4 and long-term 2050 SD5/LD5) and their input settings, including learning rates, are reported in Supplementary Note 6.1.

Skov et al.[121] report yield gains of 20.5% and 9.3% under basalt amendment on direct-drilled and ploughed spring oat in northeast England at an application rate of 18.9 t/ha. We take the midpoint of these two treatment effects, 15%, as a stylized uplift and value it on an Iowa corn–soy rotation at 2024 state-average yields[122], giving $5.65 per ton of rock at the Favorable 50 t/ha application rate (EB1). Crop, climate, and application rate all differ

Parameter	EB2 / ED2	Unit	Geo.	Source
WACC	8	%	US	Literature/assumption
Project duration	25	yr	–	
CDR yield (gross)	0.216 / 0.687	$t\,CO_2/t$ rock	–	[55;56]
Grain size	7 / 30	µm		[56]
Application rate	30	t/ha	Iowa	[50]
Transport distance	100	km	Iowa	
Mining CAPEX	0.55 / 0.55	\$/t rock		[55]
Mining OPEX	13.21 / 13.21	\$/t rock		[55]
Grinding fixed OPEX	14.31 / 14.31	\$/t rock		[55]
Grinding energy model	$277.78 \cdot 6.62\,P_{80}^{-1.162}$	kWh/t rock		[56]
Base electricity mix (grid / renewables)	70 / 30	%	Iowa	Model Calibration
Effective mix electricity price	0.0603	\$/kWh	Iowa	Derived from the base electricity mix
Effective mix carbon intensity	0.2744	$kg\,CO_2$/ kWh	Iowa	Model Calibration
T&S cost	0	$\$/t\,CO_2$		In-situ sequestration

Mining CAPEX/OPEX and grinding fixed OPEX: values from Strefler et al.[55]; identical for basalt and dunite.
Grinding energy: the empirical fit $6.62\,P_{80}^{-1.162}$ is in GJ/t rock (P_{80} in µm), converted at 1 GJ = 277.78 kWh.

Supplementary Table 7. ERW input assumptions. Base-case (EB2/ED2) parameter values for basalt and dunite, with units, geography, and sources. Paired values are ordered basalt / dunite.

Parameter	EB1	EB2	EB3	ED1	ED2	ED3
Rock type	Basalt	Basalt	Basalt	Dunite	Dunite	Dunite
Grain size P_{80} (μm)	6	7	8	21	30	40
Application rate (t/ha)	50	30	20	50	30	20
Transport distance (km)	50	100	150	50	100	150
Energy source	Renewables	Mix	Mix	Renewables	Mix	Mix
Co-product revenue (\$/t rock)	5.65	2.83	1.41	0	0	0

Supplementary Table 8. ERW project configurations. Rock type, grain size, application rate, transport distance, and co-product revenue across the six ERW project configurations.

from the trial, so this term is an illustrative valuation rather than a transferable agronomic estimate. The Realistic base case (EB2) assumes half of this maximum, an effective 7.5% yield gain (\$2.83/t rock), and the Conservative case (EB3) retains one quarter (\$1.41/t rock). The model converts these values to $\$/tCO_2$ by dividing by gross CDR yield. Dunite receives no agronomic co-product revenue because of potential trace-element risks.

1.1 Financial Assumptions

The four pathways use different weighted average costs of capital (WACC): BiCRS and BECCS 7%, ERW 8%, and DAC 10%. These differences reflect technology-specific risk profiles. BiCRS involves smaller, modular pyrolysis plants with shorter project cycles and established supply chains, warranting a lower WACC. ERW carries an intermediate rate reflecting near-term, low-tech deployment but uncertain MRV. DAC entails the largest, longest-lived capital projects with novel process integration and early-stage commercial scale-up risk, consistent with the highest rate in the set. BECCS is assigned the same 7% as BiCRS: it relies on commercially mature combustion and post-combustion-capture components with long-duration offtake, so it carries less first-of-a-kind technology risk than DAC, and the shared rate keeps the two biomass pathways directly comparable. Project lifetimes are 20 years for BiCRS and 25 years for BECCS. Current S-DAC and L-DAC project configurations use 15 and 20 years; the 2030 project configurations use 20 and 30 years, and both 2050 project configurations use 30 years. ERW uses a 25-year project duration determined by application cycles rather than a fixed plant lifetime.

Technology	Base project configuration	Baseline WACC (%)	LCCDR (baseline) (USD/tCO_2)	LCCDR (8%)
S-DAC	SD2 Commercial-Grid	10	491.7	449.5
L-DAC	LD2 Commercial-Grid	10	289.6	258.5
BECCS	BE1 Greenfield-Wood	7	89.4	94.9
BiCRS	BC2 Realistic-Wood	7	107.1	110.9
ERW Basalt	EB2 Basalt-Realistic	8	260.3	260.3
ERW Dunite	ED2 Dunite-Realistic	8	47.8	47.8

Supplementary Table 9. Harmonized-WACC check. Base-project configuration LCCDR at each pathway's baseline WACC versus a common 8% WACC. Values are recalculated under the reported investor-break-even convention.

Table 9 re-evaluates the six base project configurations at a common WACC of 8%, while retaining technology-specific lifetimes. Harmonization moves the capital-intensive DAC project configurations down by \$31–\$42/tCO_2 and the biomass pathways up by \$3.9–\$5.5/tCO_2, while ERW is unchanged. The broad ordering is stable, although L-DAC (\$258.5/tCO_2) narrowly moves below ERW Basalt (\$260.3/tCO_2). Table 2 and the sensitivity analysis in Supplementary Note 3 provide complementary robustness checks.

2 Policy Context and Market Prices

This section collects supporting policy and market context for the main cost results, including details on the 45Q production tax credit and recent CDR transaction prices observed in voluntary carbon markets.

End Use	Previous Amount ($/t$CO_2$)	IRA Amount ($/t$CO_2$)	With Multiplier (5x) ($/t$CO_2$)
Traditional CC: CO_2 Used or Utilized	36	12	60
Traditional CC: CO_2 Sequestrated	50	17	85
DAC: CO_2 Used or Utilized	35	26	130
DAC: CO_2 Sequestrated	50	36	180

Supplementary Table 10. Production Tax Credits for Carbon Capture (45Q)[14].

Because LCCDR embeds available policy support as co-product revenue, Supplementary Table 11 isolates the 45Q contribution for the eligible pathways and reports the policy-free net cost. The 45Q credit is the levelized value of the 12-year statutory credit window, discounted and re-annualized over the project lifetime (see Methods); because it is paid per ton of CO_2 captured and geologically stored, the levelized credit is essentially constant across project configurations that share a policy vintage ($78/t$CO_2$ pre-tax equivalent for the BECCS cases). DAC has no marketable co-product, so once the 45Q credit is removed its policy-free LCCDR equals LCCDR$^+$; BECCS additionally earns electricity co-product revenue, which is retained in both columns. BiCRS and ERW are treated as not 45Q-eligible at the project configuration boundary, so their policy-free cost equals the LCCDR reported in Table 2 and they are omitted here.

Without 45Q, BECCS BE1 rises from $89 to $171/t$CO_2$ and loses its base-case edge over BiCRS BC2 ($107). The low-cost, low-leakage end (ERW dunite) and the high-cost end (Frontier DAC) are unchanged by the removal of 45Q. Procurement comparisons across jurisdictions with different support regimes should therefore take policy dependence explicitly into consideration.

Technology	ID	LCCDR	45Q credit ($/t$CO_2$)	LCCDR (no 45Q)
S-DAC	SD1 Frontier	1076	−341	1416
S-DAC	SD2 Commercial-Grid	492	−305	796
S-DAC	SD3 Renewable-Coupled	426	−268	694
L-DAC	LD1 Frontier	671	−278	950
L-DAC	LD2 Commercial-Grid	290	−260	549
L-DAC	LD3 Renewable-Coupled	245	−231	476
BECCS	BE1 Greenfield-Wood	89	−82	171
BECCS	BE2 Greenfield-CropResidue	109	−84	193
BECCS	BE3 Greenfield-EnergyCrop	123	−84	207

Supplementary Table 11. 45Q policy-support exclusion. For each 45Q-eligible project configuration, the table shows LCCDR, the levelized 45Q credit at its effective per-net-ton value CPR, and the policy-free LCCDR (no 45Q). The statutory 45Q credits of \$180/tCO_2 (DAC) and \$85/tCO_2 (BECCS) are fixed per ton captured and stored. Once levelized, tax-adjusted, and allocated over net removal, they are worth more per net ton as leakage rises. Values are derived in this work (see Methods); BiCRS and ERW are not (currently) 45Q-eligible.

2.1 Observed Market-Price Data

We use the 2025 data of disclosed CDR.fyi transactions[19]. Transaction volumes and commitments (Figure 1) reflect a January 2026 snapshot of the CDR.fyi database. The disclosed-price sample underlying Figure 7 was retrieved in March 2025, as later snapshots did no longer contain price information. We remove fully duplicated records and observations without a disclosed positive price, a positive purchased volume, or a method that maps to one of the four pathways. The transaction price per ton equals the disclosed contract value divided by purchased volume. We group biochar carbon removal, biomass direct storage, and bio-oil sequestration as BiCRS; map reported BECCS and DACCS transactions to BECCS and DAC; and group enhanced weathering and mineralization methods as ERW. To limit the influence of extreme disclosed values, we winsorize the pooled price distribution at its 1st and 99th percentiles. Figure 7 estimates densities on log prices both with purchased volume as the weight and without weights, so that the second panel assigns equal weight to each transaction.

3 Sensitivity Analysis

Supplementary Figure 1 reports a one-at-a-time robustness check using the ranges in Supplementary Table 12. The ranges are literature-anchored where a published interval is available and otherwise labeled explicitly as project-finance, project-availability, logistics, cost-estimate, or market-price assumptions. We observe that plant cost and capacity factor dominate DAC costs. Capacity factor, plant cost, and biomass feedstock cost dominate BECCS. Plant cost and capacity factor dominate BiCRS. ERW remains governed primarily by the grain-size/weathering-yield trade-off. This check goes in a different direction from Figure 7. Here we change one input at a time around the base configuration per pathway. Its endpoints diagnose the main cost drivers. Varying them together could lead to a further overlap with observed prices.

Supplementary Table 12. Ranges for parameter sensitivity. Low and high values are one-at-a-time stress points, not confidence bounds or joint scenarios. Sources are cited where a published range is used; otherwise the row is explicitly labeled as a configuration or financing assumption.

Case	Parameter	Low	Base	High	Basis
S-DAC SD2	Cost of capital	7%	10%	12%	project-finance assumption; see Supplementary Table 9
S-DAC SD2	Plant cost	0.70x	1.00x	1.35x	[17;22]
S-DAC SD2	Variable cost	0.70x	1.00x	1.40x	[17;22]
S-DAC SD2	T&S cost	$10	$21	$35	[115]
S-DAC SD2	Capacity factor	65%	85%	95%	project-availability assumption
L-DAC LD2	Cost of capital	7%	10%	12%	project-finance assumption; see Supplementary Table 9
L-DAC LD2	Plant cost	0.70x	1.00x	1.35x	[17;22]
L-DAC LD2	Variable cost	0.70x	1.00x	1.40x	[17;22]
L-DAC LD2	T&S cost	$10	$21	$35	[115]
L-DAC LD2	Capacity factor	65%	85%	95%	project-availability assumption
BECCS BE1	Plant cost	0.80x	1.00x	1.25x	[115]
BECCS BE1	Biomass cost	$50	$75	$103	biomass-price stress assumption; the high endpoint reflects EU forest-residue pricing
BECCS BE1	Upstream emissions	0.80x	1.00x	1.20x	±20% feedstock carbon-intensity stress, informed by the delivered woody-residue range, around the component-built base of 40.8 $kgCO_2e$/dry t
BECCS BE1	Capture efficiency	85%	90%	95%	[115]
BECCS BE1	Capacity factor	65%	84%	90%	project-availability assumption
BiCRS BC2	Plant cost	0.75x	1.00x	1.35x	engineering cost-estimate assumption
BiCRS BC2	Feedstock cost	$27	$36	$45	feedstock-price assumption (±25% on the base value)
BiCRS BC2	Feedstock emissions	0.50x	1.00x	2.00x	feedstock-logistics assumption
BiCRS BC2	Biochar revenue	$50	$100	$150	market-price stress assumption
BiCRS BC2	Capacity factor	65%	90%	95%	project-availability assumption
ERW Basalt EB2	Cost of capital	5%	8%	10%	project-finance assumption; see Supplementary Table 9
ERW Basalt EB2	Plant cost	0.75x	1.00x	1.40x	[56]
ERW Basalt EB2	Grain size	5	7	10	[56]
ERW Basalt EB2	Transport distance	50	100	250	regional-logistics assumption
ERW Basalt EB2	CDR yield	0.70x	1.00x	1.30x	[55;56]
ERW Dunite ED2	Cost of capital	5%	8%	10%	project-finance assumption; see Supplementary Table 9
ERW Dunite ED2	Plant cost	0.75x	1.00x	1.40x	[56]
ERW Dunite ED2	Grain size	20	30	50	[56]
ERW Dunite ED2	Transport distance	50	100	250	regional-logistics assumption
ERW Dunite ED2	CDR yield	0.70x	1.00x	1.30x	[55;56]

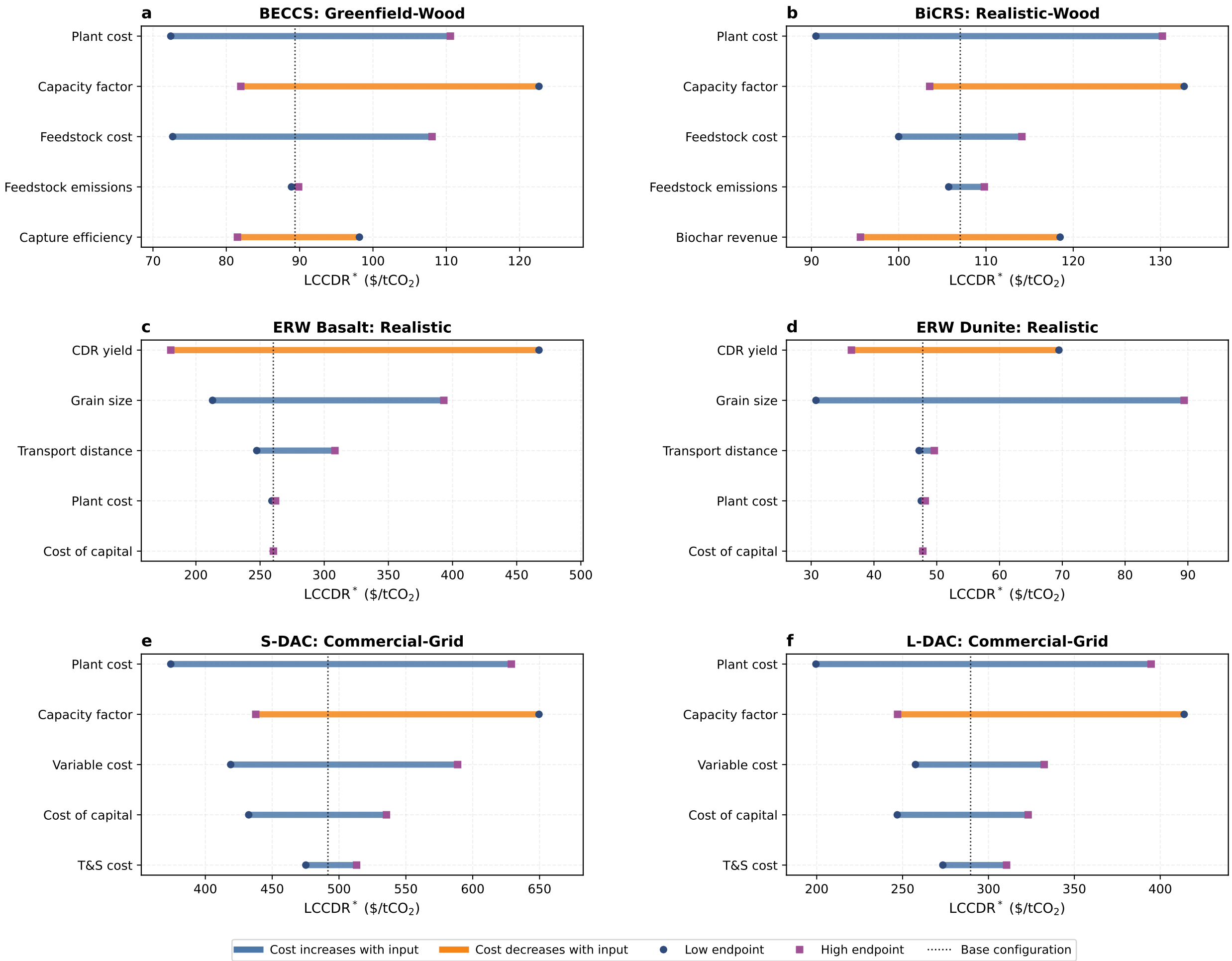

Supplementary Figure 1. Sensitivity of LCCDR. Each panel shows the LCCDR response to the low and high endpoint for each parameter in Supplementary Table 12, changing one input at a time. Bars are colored by the sign of the parameter–cost relationship (blue: net cost *rises*; orange: net cost *falls* as the input increases). Circles and squares mark the low and high input endpoints, and the dotted vertical line marks the base value.

4 Biomass Sensitivities

4.1 Biogenic Carbon Accounting

The standard convention treats biogenic carbon released without capture (uncaptured biomass-combustion flue gas for BECCS, syngas-combustion CO_2 for BiCRS) as carbon-neutral, consistent with the biomass having drawn the same carbon from the atmosphere during growth. The variant leakage factor α_{bio} re-includes these flows in the attributable-emissions total. Re-including them raises α from 4.6–7.2% to 14.1–16.4% across the BECCS project configurations and from 4.9–11.2% to 24.8–38.1% for BiCRS, lifting the corresponding LCCDR by \$10–\$14/tCO_2 (BECCS) and \$26–\$71/tCO_2 (BiCRS). Supplementary Figure 2 visualizes the shift for each project configuration.

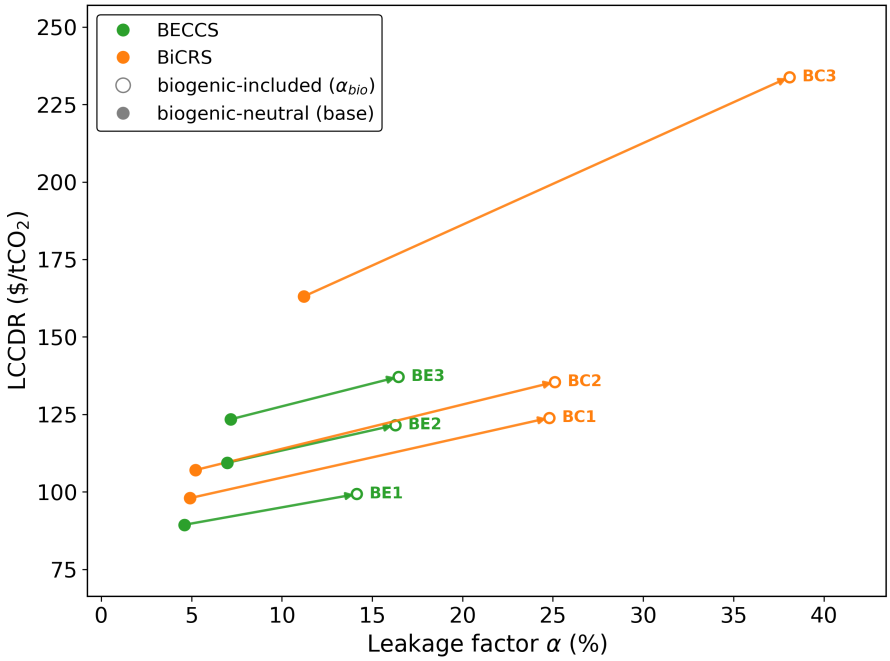

Supplementary Figure 2. Effect of the biogenic carbon-accounting boundary. For each BECCS (green) and BiCRS (orange) project configuration, the arrow runs from the biogenic-neutral base case (α) to the full biogenic-included accounting (α_{bio}). It indicates the increase in the leakage factor α and the net cost LCCDR that results from counting the uncaptured biogenic CO_2 produced when the biomass is combusted.

4.2 Higher Biomass Carbon Intensity

Next we examine how raising the biomass upstream carbon intensity impacts LCCDR and LCCDR$^+$. Supplementary Figure 3 portrays BE3 energy-crop (miscanthus) and BC3 crop-residue (corn stover) cases. Holding each case's cost base fixed, both LCCDR and LCCDR$^+$ rise convexly with the upstream carbon intensity and diverge as the net-removal denominator $(1-\alpha)$ approaches zero. The reported base cases sit well to the left of this rise, so both retain a large margin before net removal collapses; that margin is what a potential counterfactual land-use boundary erodes for the energy-crop cases. The figure also shows that, absent policy support, low-carbon feedstocks are more economically processed via BiCRS and high-carbon feedstocks via BECCS. The crossover point is around 348 $kgCO_2e$/dry t (19 gCO_2e/MJ), which is well above the base-case corn-stover and miscanthus values.

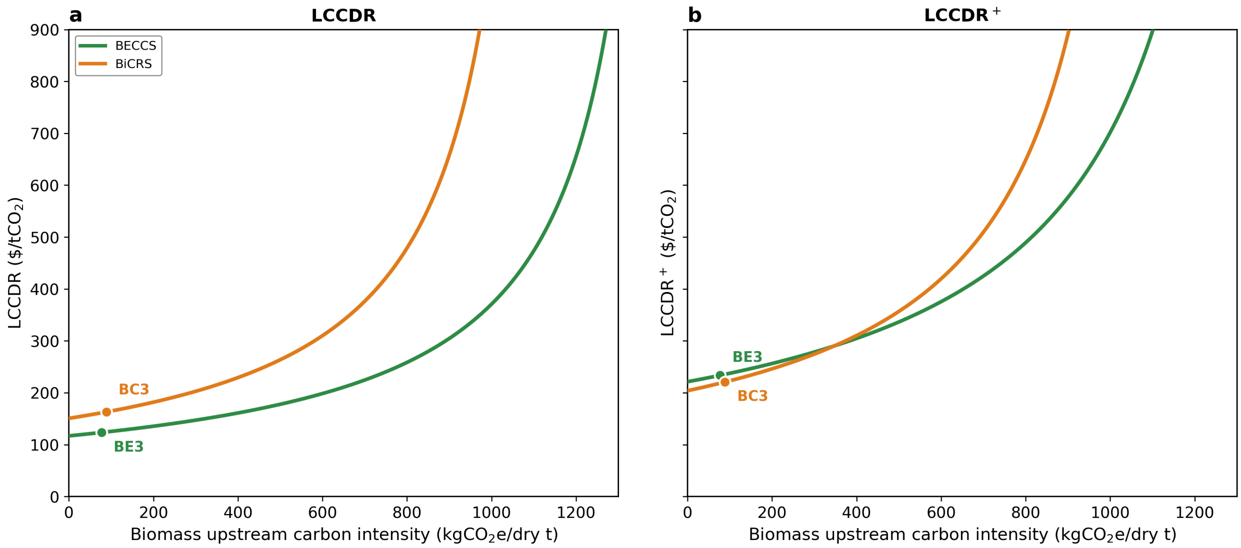

Supplementary Figure 3. LCCDR response to biomass upstream carbon intensity. Main-case LCCDR (**a**) and LCCDR$^+$ (**b**) for the BE3 energy-crop (miscanthus, BECCS) and BC3 crop-residue (corn stover, BiCRS) cases, as biomass upstream carbon intensity increases. Markers denote the reported base cases.

4.3 Energy-Crop Land-Use Change

Our LCCDR metric excludes counterfactual debits and credits by design (see section 2). To show the effect of this boundary choice, we quantify the potential impact for the single most exposed project configuration: BE3 EnergyCrop (dedicated miscanthus), the only project configuration in the main analysis that could plausibly displace food or carbon stocks. We add an indirect land-use-change (iLUC) debit on top of the base cultivation/harvest/transport emissions (76.9 kgCO_2e/dry t), holding every other BE3 input fixed. Because the BECCS model charges upstream emissions per dry ton of biomass, we convert literature iLUC factors using the workbook-calibrated miscanthus higher heating value (19.16 GJ/t), so 1 gCO_2e/MJ corresponds to 19.16 kgCO_2e/dry t. The debit raises the leakage factor α and therefore both LCCDR$^+$ and LCCDR.

iLUC counterfactual	iLUC debit (gCO_2e/MJ)	Total upstream (kgCO_2e/dry t)	α (%)	LCCDR (\$/tCO_2)
Marginal / low-iLUC-risk land (base)	0	76.9	7.2	123
Grassland direct LUC (modest)	10	268.5	20.0	143
Cropland iLUC (mid range)	30	651.7	45.7	211
Cropland iLUC (high)	50	1034.9	71.4	401
Net-removal threshold $\alpha = 100\%$ at ≈ 72 gCO_2e/MJ				

Supplementary Table 13. Counterfactual iLUC debit on BECCS energy-crop configuration. The iLUC debit is added to the base upstream emissions (76.9 kgCO_2e/dry t) and converted at the miscanthus HHV (1 gCO_2e/MJ = 19.16 kgCO_2e/dry t). All other BE3 inputs are held at their main values. Beyond a debit of ~72 gCO_2e/MJ (~1,460 kgCO_2e/dry t total upstream) the leakage factor reaches 100%.

Three points follow. First, the result is robust to a modest penalty. Siting on marginal or degraded land can reduce displacement risks. The EU Renewable Energy Directive (RED II) provides criteria for classifying some biomass as "low-iLUC-risk". BE3 then stays close to its main \$123/tCO_2. Even a modest grassland direct-LUC debit of 10 gCO_2e/MJ leaves BE3 at \$143/tCO_2, still far below DAC. Second, the exposure becomes material under a cropland-displacement counterfactual. At 50 gCO_2e/MJ (within the 95% interval of Plevin et al.[123] for food-crop iLUC), α reaches 71% and LCCDR rises to \$401/tCO_2, above the L-DAC commercial case. Third, the net-removal denominator $(1-\alpha)$ reaches zero at an iLUC debit of roughly 72 gCO_2e/MJ; beyond this the energy-crop configuration emits more than it sequesters. The central and upper food-crop iLUC estimates from the biofuel literature, namely ~104 gCO_2e/MJ for corn ethanol[124] and an upper bound near 340 gCO_2e/MJ[123], with one-time grassland-conversion carbon debts on the order of 130 tCO_2/ha[125], all lie above this threshold. This shows that a single unverifiable counterfactual could swing the energy-crop project configuration from a \$123/tCO_2 removal to a net emitter depending on an assumed siting that audited markets cannot confirm. The same logic applies symmetrically to credits, where we likewise exclude the residue-diversion avoided-decomposition credit that would *lower* BiCRS and crop-residue BECCS costs, which we consider a promising area for future research.

4.4 Bio-oil-only Credit Eligibility

The main BiCRS results assume that the permanence adjusted biochar and all geologically injected bio-oil are both eligible for removal credits. We test an alternative market boundary in which only bio-oil is credit-eligible. The physical system is unchanged: biochar is still produced, transported, applied, and sold as a soil product. Its sales remain a co-product revenue stream, and all project costs and attributable emissions remain within the vertically integrated boundary. This changes the price that must be earned on each bio-oil ton sold for the project to break even.

Project configuration	Credited removal	α (%)	LCCDR^- ($/net credited tCO_2)	LCCDR	LCCDR^+
Favorable-Wood	Both streams	4.91	93.2	98.0	129.5
	Bio-oil only	10.01	189.8	210.9	278.7
Realistic-Wood	Both streams	5.22	101.5	107.1	138.6
	Bio-oil only	10.64	206.7	231.3	299.5
Conservative-Residue	Both streams	11.21	144.8	163.0	220.7
	Bio-oil only	21.52	278.1	354.3	479.6

Supplementary Table 14. BiCRS sensitivity to bio-oil-only credit eligibility. This table reports the effect of crediting bio-oil only under a slow pyrolysis setting, as in the three project configurations. Bio-oil-only rows report prices per net credited bio-oil ton while retaining physical biochar sales revenue and all integrated-project costs and emissions.

Restricting eligibility to bio-oil raises the break-even credit price by 115–117% across the three project configurations. For Realistic-Wood, the price increases from $107 to $231 per net credited ton. Its gap relative to the $89/$tCO_2$ BECCS Wood base case LCCDR would then widen from $18 to $142 per ton.

5 Hourly Electricity Prices and Operating Schedules

The main calculations summarize operation using technology-specific annual capacity factors. This note tests whether hourly electricity prices alter that simplification for DAC, where electricity is an operating cost, and BECCS, where electricity is a co-product.

5.1 DAC hourly utilization

For DAC, we solve the utilization choice over the hourly grid-price vector to optimize the lowest investor break-even removal price. The contribution margin remains positive for far more hours than the maintenance-constrained operating schedule permits. The optimizer therefore selects the maximum technically achievable utilization, and price-responsive curtailment does not change the reported LCCDR.

5.2 BECCS hourly-price diagnostic

The BECCS Wood base case values electricity co-product revenue at an annual-average wholesale price of \$44/MWh. We test this convention against an 8,760-hour Texas wholesale price vector[120] for 2015–2024, which has a mean of \$46.8/MWh. Under constant baseload utilization the co-product revenue can be simplified via the mean price. The higher mean of the hourly vector therefore lowers LCCDR via the co-product revenue by \$1.47/tCO_2 net relative to the \$44/MWh base case; the hourly price shape has no separate effect under constant output.

We then impose a simple revenue-timing diagnostic. We assume that the plant operator is a price taker with perfect foresight and concentrates electricity sales in the top 90% of price hours, thereby assigning required downtime to the lowest-price hours. Removal volumes, variable costs, and capacity charges remain at their base-case values. In this case, the LCCDR falls by \$5.15/tCO_2 net relative to the base case. We do not interpret this calculation as an optimal BECCS dispatch schedule. The model does not resolve start-up costs or ramping constraints at hourly resolution, so a formal dispatch optimum would imply more operational precision than the current calibration supports. But the diagnostic suggests that, under current market prices, the hourly pattern of electricity revenue would not materially change BECCS operation. We note that this may change in the future, under more volatile market prices and in particular with more hours with negative prices.

At \$44/MWh, electricity revenue lowers BECCS Wood LCCDR by \$24.52/tCO_2 net. The levelized 45Q credit lowers it by \$81.77/tCO_2 net. Together they provide a \$106.30/tCO_2 revenue offset and reduce LCCDR from \$195.67 without co-product or policy revenue to \$89.37. The tax credit accounts for 77% of this offset and electricity revenue for 23%. Supplementary Figure 4 shows this split across electricity prices. The small hourly-price effects therefore do not imply that electricity revenue is unimportant for BECCS. They show that replacing the annual-average price with an hourly pattern, and concentrating revenue in the higher-priced hours, does not materially change the base-case result.

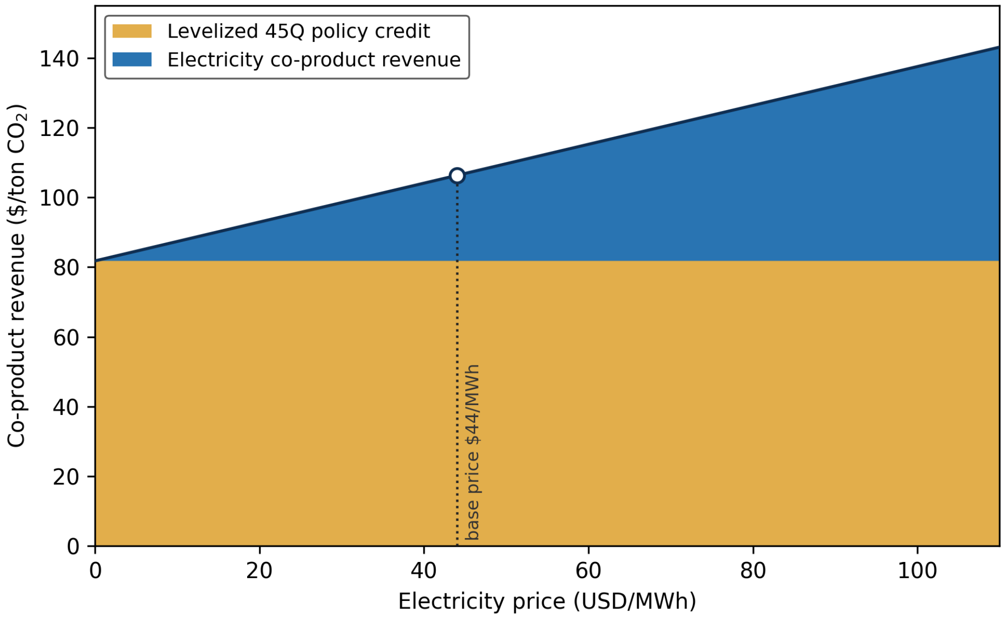

Supplementary Figure 4. BECCS co-product revenue across electricity prices. Electricity co-product revenue increases linearly with the electricity price when electricity output per net ton of removal is held fixed. The levelized 45Q credit is independent of the electricity price.

6 Cost Dynamics

Cost evolution is pathway-specific. We apply prospective learning to DAC, where repeated plant deployment can plausibly reduce equipment and fixed operating costs, specifically for modular S-DAC plants. For ERW, BECCS, and BiCRS, the more defensible near-term dynamics concern changing inputs: grinding electricity for ERW, and feedstock, logistics, and process integration for the biomass pathways. We therefore report a controlled ERW clean-grid diagnostic below but do not impose generic technology-wide learning curves on BECCS or BiCRS.

6.1 Future DAC Configurations

Supplementary Table 16 separates four modeled configurations per DAC chemistry for a 1 Mt CO_2/yr plant. The current configurations are SD2/LD2 with commercial-grid power and SD3/LD3 with coupled renewables. The dated configurations are SD4/LD4 for the mature 2030 case and SD5/LD5 for 2050; SD5 is all-electric, whereas LD5 retains natural-gas heat with capture. SD3/LD3 isolates a cleaner energy supply without changing the plant architecture. SD4/LD4 and SD5/LD5 jointly change learning, process performance, energy supply, project life, and T&S scale (Supplementary Table 15). The 45Q credit is active in the current and 2030 configurations and assumed to expire by 2050 ($CPR = 0$); LCCDR^{+} therefore provides the consistent policy-free comparison.

Parameter	SD4/LD4 (Mature-2030)	SD5/LD5 (Long-term 2050)
Forecast Horizon	2030	2050
Cost assumption	base	base
Process energy inputs	Electricity + thermal	Electricity / Electricity + thermal
Electricity source	Grid	Wind & Solar
Thermal source	Natural Gas	— / Natural Gas
Grid Connection	Yes	Yes
Nameplate Capacity (Mt/yr)	1.0	1.0
T&S cluster size	Medium	Large
Learning Rates	0.12 / 0.08	0.12 / 0.08

Supplementary Table 15. Future-horizon DAC input settings. Input assumptions for the Mature-2030 (SD4/LD4) and long-term 2050 (SD5/LD5) DAC project configurations, complementing the current-project-configuration inputs in Supplementary Table 6. In the 2050 column, entries of the form "S-DAC / L-DAC" mark where the chemistries differ: SD5 is all-electric on Wind & Solar, whereas LD5 retains captured natural-gas calcination heat. Learning rates are prospective experience rates for capacity and fixed O&M[22].

In the following cost build-ups, the levelized cost of capture (LCOC) is the gross plant-gate cost before transport and storage; adding s gives the reported gross cost.

The apparent increase from LD4 (LCCDR \$111) to LD5 (\$207) is policy-driven: LCCDR^{+} falls from \$313 to \$207 after 45Q expires, not enough to offset the net 45Q effect. The configuration comparison also shows why the paths should not be read as a pure learning curve. Renewable coupling lowers both cost and leakage at SD3/LD3, while the dated cases additionally change equipment cost, efficiency, lifetime, and T&S scale. Two drivers move the main cost down between Current and 2050: (i) experience-curve learning on capacity cost (c), and (ii) a cleaner electricity supply that shrinks the leakage factor α.

High-temperature heat is a separate L-DAC design choice. Holding all other LD5 assumptions fixed, retained natural gas with capture is the lowest-cost option, while concentrated solar heat delivers the lowest modeled leakage at substantially higher cost. A residual

in $/tCO$_2$	S-DAC: Solid Sorbent			
	SD2 Commercial-Grid	SD3 Renewable-Coupled	SD4 Mature-2030	SD5 Long-term-2050
Cost of capacity, c^g	264.09	264.09	109.38	63.64
Fixed operating cost, f^g	79.71	79.71	33.01	19.21
Variable operating cost, w^g	159.64	154.13	124.39	75.61
Transport & storage cost, s^g	20.90	20.90	10.27	7.35
Gross cost, LCOC $+ s$	524.34	518.83	277.05	165.81
Leakage factor, α	34.16%	25.26%	24.39%	8.96%
LCCDR$^+$	796.42	694.19	366.43	182.13
Effective 45Q per net ton	−304.70	−268.41	−231.31	0.00
LCCDR	491.72	425.78	135.12	182.13

in $/tCO$_2$	L-DAC: Liquid Solvent			
	LD2 Commercial-Grid	LD3 Renewable-Coupled	LD4 Mature-2030	LD5 Long-term gas+CCS
Cost of capacity, c^g	207.08	207.08	118.84	84.92
Fixed operating cost, f^g	69.95	69.95	40.15	28.69
Variable operating cost, w^g	72.14	62.83	67.14	54.57
Transport & storage cost, s^g	20.90	20.90	10.27	7.35
Gross cost, LCOC $+ s$	370.07	360.76	236.40	175.53
Leakage factor, α	32.61%	24.17%	24.45%	15.03%
LCCDR$^+$	549.12	475.77	312.90	206.57
Effective 45Q per net ton	−259.51	−230.65	−201.89	0.00
LCCDR	289.62	245.13	111.02	206.57

Supplementary Table 16. LCCDR across DAC configurations. SD3/LD3 adds the Renewable-Coupled configuration to the Commercial-Grid, Mature-2030, and long-term 2050 cases. The 2050 L-DAC case retains captured natural-gas calcination heat; SD5 is all-electric. T&S cluster size scales from Small to Medium and Large in the dated configurations. The effective 45Q row reports CPR; the credit is active in the current and 2030 configurations and expires by 2050. Cost components here are on the gross-capture basis; c^g is the tax-adjusted capacity cost, so the four gross components sum to the gross cost. The per-net components in Table 1 follow by dividing each by $(1 - \alpha)$. All $LCCDR$ terms are equivalent to the main body specification.

upstream-methane leakage keeps LD5's α at 15%, above S-DAC's all-electric 2050 case (9%), which is why SD5 ($182) remains below LD5 despite S-DAC's higher present-day cost. The all-electric option is not automatically the lowest-leakage case for L-DAC because supplying the full calcination load increases electricity-related upstream emissions.

Beyond the forecast-horizon trajectory, the renewable-coupling lever can be isolated at the current project configurations: Figure 6 plots the post-T&S leakage factor α against LCCDR for all five DAC project configurations and shows that the Renewable-Coupled

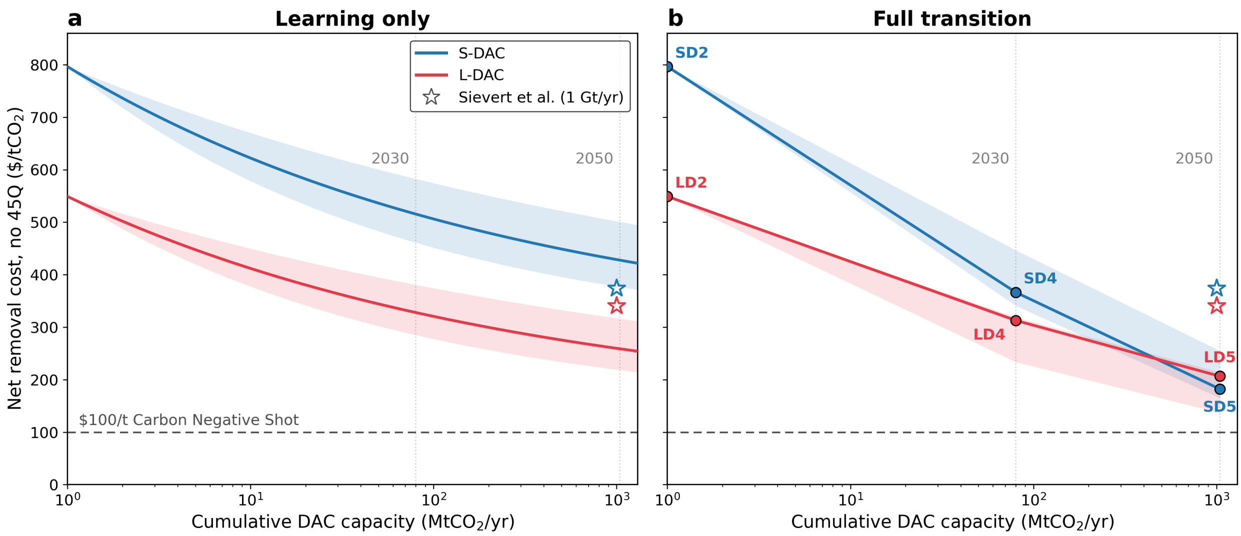

Supplementary Figure 5. Future DAC Cost Dynamics Panel (**a**) shows the effect of an 8–15% learning-rate to capacity and fixed operating costs for the base-cases, holding all other variables fixed. Panel (**b**) connects the policy-free LCCDR$^+$ values of the Commercial-Grid, Mature-2030, and long-term 2050 configurations. It combines learning with process, energy, lifetime, and T&S changes. Cumulative deployment follows the IEA-base estimates of 1, 80, and 1,041 Mt[8]. Stars show the component-based estimates of Sievert et al. at 1 $GtCO_2$/yr[22]; the dashed line marks the U.S. Carbon Negative Shot target[13].

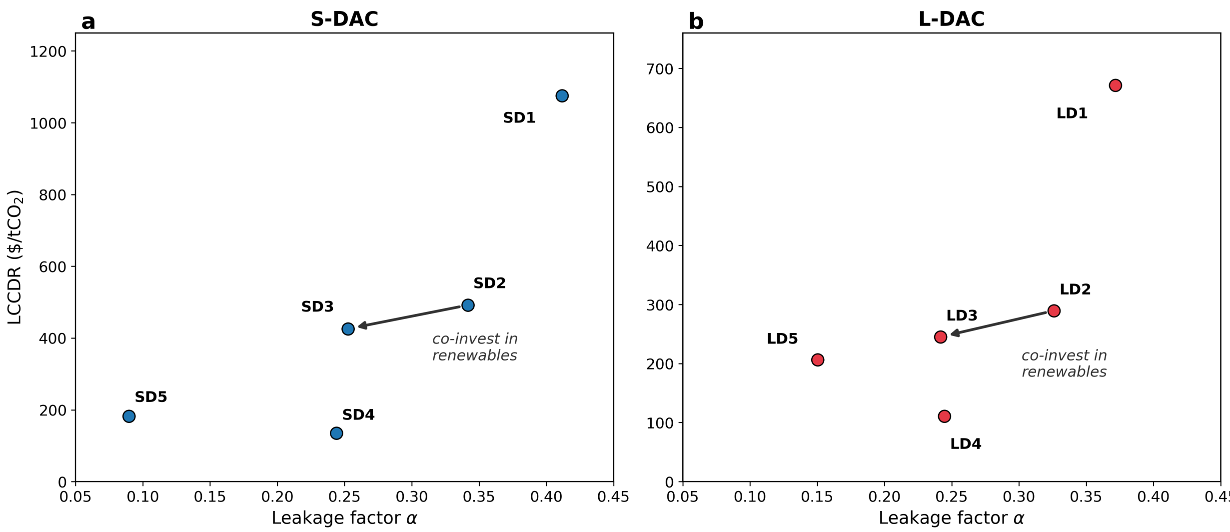

Supplementary Figure 6. Cost-vs-leakage trade-off across DAC projects. This figure shows α against LCCDR for the five DAC project configurations, separately for S-DAC (**a**) and L-DAC (**b**).

SD3/LD3 configuration sits below and to the left of the grid-only SD2/LD2 base: both cheaper and cleaner per net ton of removed CO_2.

6.2 ERW Grinding Electricity

For ERW, grid decarbonization acts through the emissions denominator rather than a generic equipment-learning curve. Supplementary Table 17 sets grinding-electricity emissions to zero while holding electricity price, rock properties, application rate, transport, co-product revenues, and finance fixed. The resulting change is large for realistic basalt because fine grinding is electricity-intensive, but small for realistic dunite under its higher modeled gross removal yield.

	α		LCCDR ($/t$CO_2$)		Change
Project configuration	Base grid	Zero-emission grid	Base grid	Zero-emission grid	$/t$CO_2$
EB2 Basalt-Realistic	32.28%	7.97%	260.32	191.55	−68.77
ED2 Dunite-Realistic	3.92%	2.51%	47.78	47.08	−0.69

Supplementary Table 17. Controlled ERW clean-grid diagnostic. Only the emissions intensity of grinding electricity changes, from 0.2744 to 0 kgCO_2e/kWh; the electricity price remains $0.0603/kWh and all other inputs are fixed. The calculation is an emissions-intensity sensitivity, not a dated forecast and not an assumption of zero-cost electricity.

7 ERW Sensitivities

7.1 Deployment Conditions and Regional Effects

The ERW model does not resolve climate and soil conditions separately. Instead, these conditions enter through the fixed weathering-rate constants. The constants adopted from Strefler et al.[55] are reported for pH 7 and 25 °C. Our reported project configurations are based on those reference-rate constants. We assume sufficient water availability throughout the year as another deployment condition.

Within the continental United States, South Florida provides a close climatic analogue for the temperature assumption. The 1991–2020 normal at Miami International Airport is 25.3 °C, with annual precipitation of 1,712 mm[126]. These conditions are close to the reference temperature and humidity necessary, but naturally can only hint at site-specific dissolution performance. Outside of the U.S., countries such as Brazil, Indonesia, and Malaysia exhibit similarly suitable temperature and precipitation conditions.

For more realistic regional deployment, Strefler et al. also provide estimated adjustment factors for the reference constants[55]. They derive regional factors of 0.95 for their warm class and 0.35 for their temperate class from an Arrhenius adjustment normalized to 25 °C. The calculation uses a common activation energy of 50 kJ/mol and annual mean air temperatures of 24.3 °C and 10.2 °C, respectively. These simple bioclimate categories are based on growing degree days and aridity. We use these factors as sensitivity diagnostics.

Project configuration	25 °C reference factor 1.00	Warm-region factor 0.95	Temperate-region factor 0.35
	LCCDR (USD/tCO_2)		
EB1 Basalt-Favorable	125.1	132.0	384.7
EB2 Basalt-Realistic	260.3	281.1	6,485.3
EB3 Basalt-Conservative	340.1	370.1	No net removal
ED1 Dunite-Favorable	28.9	30.4	84.0
ED2 Dunite-Realistic	47.8	50.4	147.7
ED3 Dunite-Conservative	70.4	74.4	231.6

Supplementary Table 18. ERW temperature-rate diagnostic. LCCDR is recalculated after multiplying the weathering-rate constant by the regional factors[55]. Grain size and all cost, emissions, logistics, and co-product inputs remain fixed at their reported project-configuration values. The 1.00 column contains the unchanged main estimates. The other columns are sensitivities, not rebased results or complete regional calibrations.

The warm-region factor raises LCCDR by 5–9% across the six configurations, leaving the interpretation of the current reference-rate results largely unchanged for a warm and humid deployment. The temperate factor has a much larger effect. The dunite range rises from \$29–\$70 to \$84–\$232/tCO_2. For basalt, the fixed process emissions become large relative to gross removal: Basalt-Realistic retains only a small positive net-removal denominator, while Basalt-Conservative becomes net-emitting. The resulting cost response is therefore nonlinear.

Temperature alone does not determine land suitability. Precipitation seasonality, soil type, irrigation, and the crop cycle can alter dissolution and carbon export under otherwise similar temperature conditions[127]. The model also does not price land rent, farmer compensation, irrigation, or site-specific monitoring. Warm and humid conditions make the reference-rate assumption plausible, but do not guarantee that it will be realized. Conversely, we do not model a regional LCCDR for arid or semi-arid sites because a temperature-only adjustment would omit their hydrological constraints. Supplementary Figure 8 below examines how lower realized field rates affect the dunite economics.

7.2 Grain Size

Grain size is a decision variable with two opposing effects: finer grinding raises the specific surface area and the modeled dissolution fraction ω (more gross removal per ton of rock), but is more electricity-intensive, so grinding cost and its attributable emissions rise.

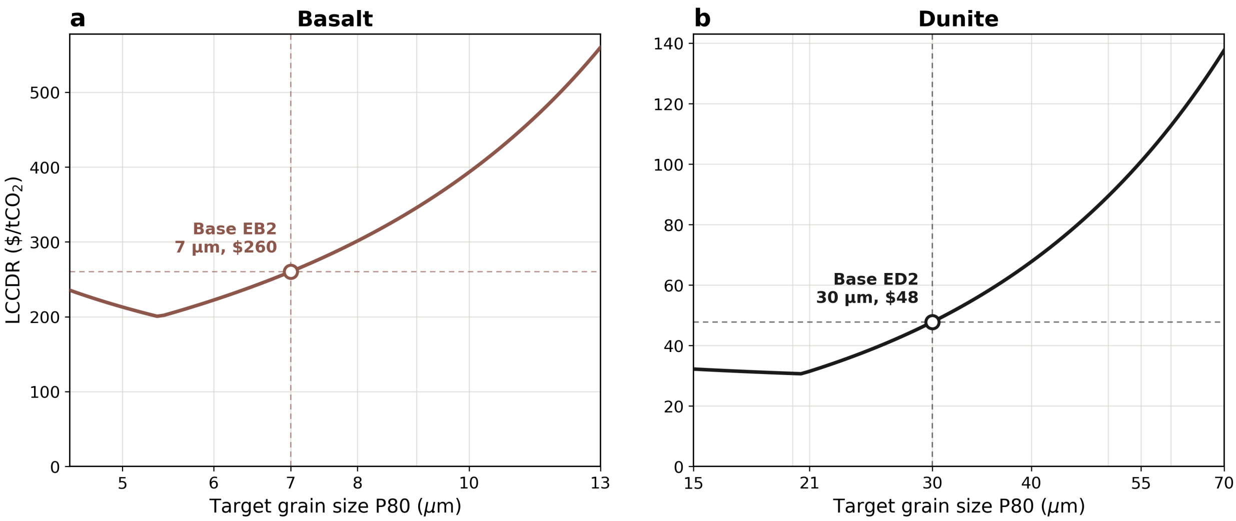

Supplementary Figure 7. ERW grain-size sensitivity. LCCDR for the realistic base case of each rock (basalt EB2, dunite ED2) as the target grain size P_{80} varies, all other inputs held fixed. Finer grinding raises the modeled dissolution fraction and gross yield but is electricity-intensive; the credited first-year uptake is capped at the stoichiometric ceiling ($\omega \leq 1$). Open markers and dashed lines mark the base cases (EB2 at 7 μm, ED2 at 30 μm).

Figure 7 sweeps the target grain size P_{80} for the realistic base case of each rock, holding all other inputs fixed. The curves reach their minimum at approximately 5.4 μm for basalt and 20.5 μm for dunite. Below these thresholds, the cap $\omega \leq 1$ prevents additional credited first-year uptake, so finer grinding only adds energy cost and emissions. Basalt is far more grain-sensitive than dunite because its lower stoichiometric sequestration potential (0.3 versus 1.1 tCO_2/t rock) leaves a smaller net-removal denominator. Costs therefore rise steeply as coarser grinding lowers the yield. The base cases (EB2 at 7 μm, ED2 at 30 μm) sit close to these cap-binding points.

7.3 Dunite Weathering Rates

The ED1, ED2, and ED3 LCCDR figures in Table 2 depend on the assumed weathering-rate constant. We therefore evaluate three alternative weathering-rates. The *Lower-rate bound* uses the lower pH-7 dunite rate from Strefler et al.[55] ($10^{-9.95}$ mol m^{-2} s^{-1}). The *Modeled rate* is the default used for the main results ($10^{-9.86}$ mol m^{-2} s^{-1}). The *Upper-yield cap* maps the upper ultrabasic CDR yield from Zhang et al.[56] (1.1 tCO_2/t rock), with annual dissolution capped at 100% to respect the physical ceiling. All other inputs (grain size, application rate, transport distance, energy source, taxes, and co-product revenues) remain at each project configuration's default. The field study of Beerling et al.[50] is not used here because it reports field CDR for basalt only.

Supplementary Table 19. Dunite weathering-rate sensitivity. Lower bound uses the lower dunite rate from Strefler et al.[55]. Modeled rate is the default used for the main results. Upper-yield cap maps the upper ultrabasic CDR yield from Zhang et al.[56] (1.1 tCO_2/t rock).

Project configuration	Weathering case	Gross yield (tCO_2/t rock)	α (%)	$LCCDR^-$ (USD/tCO_2)	LCCDR	$LCCDR^+$
ED1	Lower-rate bound	0.869	1.10	35.2	35.6	35.6
ED1	Modeled rate	1.069	0.90	28.6	28.9	28.9
ED1	Upper-yield cap	1.100	0.87	27.8	28.1	28.1
ED2	Lower-rate bound	0.559	4.82	56.5	59.3	59.3
ED2	Modeled rate	0.687	3.92	45.9	47.8	47.8
ED2	Upper-yield cap	1.100	2.45	28.7	29.4	29.4
ED3	Lower-rate bound	0.391	8.15	80.9	88.0	88.0
ED3	Modeled rate	0.481	6.62	65.7	70.4	70.4
ED3	Upper-yield cap	1.100	2.90	28.7	29.6	29.6

Supplementary Table 19 shows two findings. First, the modeled low-cost, low-leakage result is robust to the assumed weathering-rate. ED1 LCCDR rises only to \$35.6/tCO_2 with $\alpha = 1.1\%$, so it remains in the low-cost, low-leakage region. At the other end, the Upper-yield cap binds at 100% annual dissolution, making ED1 essentially insensitive to rate increases beyond the modeled rate. Second, the lower-rate bound raises ED3 from \$70 to \$88/tCO_2 and increases α from 6.6% to 8.2%. Across all dunite configurations, the main-text range would therefore widen from \$29–\$70/tCO_2 to \$36–\$88/tCO_2. The ordering relative to basalt and the other technology families is preserved. This check varies the weathering-rate constant within the laboratory range reported at the reference temperature.

Supplementary Figure 8 tests lower realized field rates relative to the modeled laboratory rate. Because process emissions are fixed per ton of rock, a slower field rate lowers gross yield, raises α, and increases LCCDR. ED2 Realistic stays below the \$100 target down to 50% of the modeled rate. ED1 Favorable reaches the target at 30%, while ED3 Conservative reaches it at 72%. For ED2, fixed process emissions exceed gross removal below roughly 4% of the modeled rate.

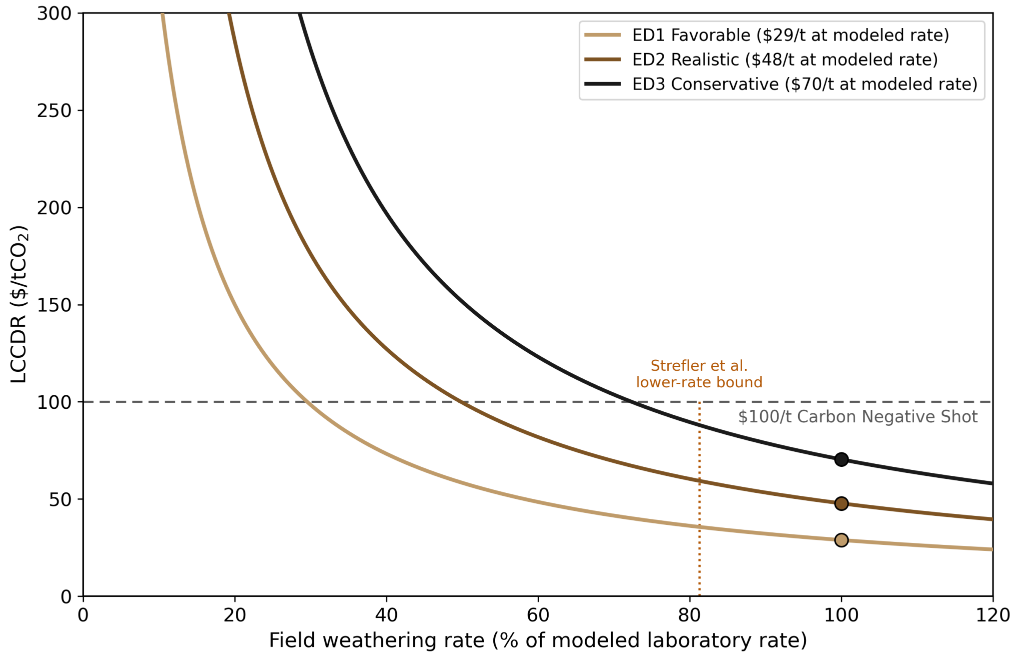

Supplementary Figure 8. Dunite LCCDR under lower field weathering rates. LCCDR for the three dunite project configurations as the field weathering rate falls below the modeled value (markers at 100%). The dashed line marks the \$100 Carbon Negative Shot target. The dotted line marks the lower-rate laboratory bound from Strefler et al.[55]. Because process emissions are fixed per ton of rock, a lower field rate raises both the leakage factor and the levelized cost.

7.4 MRV Costs

We further analyze the impact of adding specific MRV costs. Because ERW MRV costs are charged per verified net ton, the broadest cost metric adjusts accordingly: $\text{LCCDR}_{\text{MRV}} = \text{LCCDR} + m$. Public registry fee schedules report pathway- and scale-dependent verification or service fees, while ERW field MRV also depends on project-specific sampling density, analytical chemistry, and quantification uncertainty. We therefore treat $m \in \{5, 10, 20\}$ USD/tCO_2 as a stress range[103;104]. This range mirrors registry and certification fee schedules; a comprehensive field sampling and laboratory program could exceed it. Even at $m = \$20/tCO_2$, ED2 rises from \$47.8 to \$67.8/tCO_2 and remains within the low-cost region of the project configuration map.

Two further dunite-specific caveats bear on the ED1–ED3 figures: First, ultramafic rocks contain nickel and chromium that can leach into agricultural soils at gigaton-scale application rates, a trace-metal risk not present for basalt[99]. Second, the cation-versus-carbon accounting debate[98] bears specifically on faster-weathering substrates such as dunite, where MRV

Supplementary Table 20. ERW MRV cost additions for dunite. The MRV cost is applied directly to LCCDR because it is denominated per verified net ton.

Project configuration	No addition	+\$5/t	+\$10/t	+\$20/t
	LCCDR (USD/tCO_2)			
ED1	28.9	33.9	38.9	48.9
ED2	47.8	52.8	57.8	67.8
ED3	70.4	75.4	80.4	90.4

uncertainty around the gross-removal denominator is amplified relative to slower basalt deployments. Both considerations argue for reading the low-cost results as a technical-potential frontier instead of near-term deployable cost, consistent with the land-availability constraint noted in the main text.

7.5 Removal Timing

The main ERW calculation recognizes $\omega Y^{\max}$, the modeled first-year uptake per ton of applied rock, in the application year and does not credit later weathering of the residual rock. This differs from steady-state ERW assessments such as Strefler et al.[55], where the weathered share of a standing rock stock is replenished and each replacement ton is effectively valued against the full stoichiometric uptake $Y^{\max}$. We represent the main specification as a one-year crediting horizon. For the finite-horizon sensitivity, the model-implied uptake from one application in year j is instead

$$\mu_j = Y^{\max}\omega(1-\omega)^j, \qquad j = 0, 1, \ldots,$$

where ω is the modeled annual dissolution fraction and $Y^{\max}$ is the rock-specific stoichiometric CO_2-uptake ceiling per ton of rock (0.3 tCO_2/t rock for basalt and 1.1 tCO_2/t rock for dunite in our calibration). For a finite crediting and MRV horizon H, cumulative physical and present-valued gross removal are

$$q_H^{\text{phys}} = \sum_{j=0}^{H-1} \mu_j = Y^{\max}\big[1-(1-\omega)^H\big] < Y^{\max}, \qquad q_H^{\text{PV}} = \sum_{j=0}^{H-1} \mu_j \gamma^j,$$

with $\gamma = 1/(1+r)$ and the ERW WACC $r = 8\%$. Costs, co-product revenue, and attributable process emissions remain in the application year; no uptake after H is credited. The case $H = 1$ therefore reproduces the main denominator $\omega Y^{\max}$ exactly. We report $H \in$

$\{1, 5, 10, 25\}$ as the geometric schedule approaches its stoichiometric ceiling asymptotically and actual uptake may remain (considerably) below that ceiling. The long-horizon endpoint approximates the steady-state full-potential cost convention; it is therefore an upper-bound removal (lower-bound cost) check. The horizons also have a market counterpart. Registries credit ERW ex post for weathering measured in a monitoring period, under initial crediting periods of ten years that can be renewed, twice under Puro.earth and without a stated limit under Isometric[101;102;128]. $H = 10$ therefore corresponds to a single crediting period and $H = 25$ to a renewed one. Neither registry credits a modeled multi-year uptake path at application: Puro.earth permits model extrapolation only from one year to the next, and Isometric requires model re-validation on data from the preceding twelve months in every reporting period. This sensitivity isolates the crediting horizon conditional on ω; Supplementary Figure 8 separately tests lower realized field rates.

Repeated application creates a separate standing-load amount. Let A denote annual rock application per hectare. If residual rock follows the geometric cohort kinetics above, the peak unweathered stock immediately after the nth application and before that year's dissolution is:

$$M_n = A \sum_{k=0}^{n-1} (1 - \omega)^k = A \frac{1 - (1 - \omega)^n}{\omega}.$$

Cumulative throughput nA is therefore not the amount simultaneously present on the field. Over 25 years the six project configurations process 500–1,250 t/ha, but their modeled peak stocks would be only 32.7–57.3 t/ha. For EB2 and ED2, respectively, the peaks are 41.6 and 48.0 t/ha, below the 150 t/ha maintained-stock assumption used by Strefler et al.[55]. Keeping those central cases below that screening benchmark requires realized dissolution rates of at least 27.6% and 31.9% of their modeled rates. These calculations can only serve as a sensitivity: our model has no endogenous saturation feedback. Strefler's value is an assumed standing-stock limit and the four-year repeated-application trial of Beerling et al.[50] does not establish performance over a 25-year project. The check shows why cumulative throughput alone cannot establish saturation and why field realization, as discussed above, remains the binding uncertainty.

Under the current kinetic calibration, extending the horizon lowers LCCDR because the additional credited residual uptake expands the net-removal denominator by more than discounting reduces it. At $H = 5$, EB2 falls from \$260.3 to \$172.2/tCO_2 and ED2 from

Supplementary Table 21. ERW repeated-application check. Cumulative throughput is annual application multiplied by the 25-year project duration. Peak standing stock applies the geometric cohort kinetics to residual rock and is compared with the 150 t/ha maintained-stock assumption in Strefler et al.[55]. The final column is the minimum realized dissolution rate, as a share of the modeled rate.

Project	Application (t/ha/yr)	25-year throughput (t/ha)	Modeled ω (%/yr)	Peak stock (t/ha)	Minimum rate (% of modeled)
EB1	50	1,250	87.3	57.3	38.2
EB2	30	750	72.1	41.6	27.6
EB3	20	500	61.1	32.7	21.1
ED1	50	1,250	97.2	51.4	34.3
ED2	30	750	62.5	48.0	31.9
ED3	20	500	43.7	45.7	29.5

\$47.8 to \$30.9/tCO_2; changes after year 10 are negligible in the modeled schedules. The 99% thresholds span 2–9 years across the six project configurations; no complete-dissolution year is defined, and the workbook's exact-zero cells are numerical-underflow diagnostics only. The long-horizon values approach the full-potential treatment used in steady-state ERW assessments and should be read as maximum feasible removal under the modeled weathering rates at the assumed grain sizes. They are not revised main estimates: they presume continued verification and field realization of those rates. The main values retain the one-year convention, which is conservative with respect to later residual crediting but does not resolve whether the modeled application-year rate is achieved in the field.

Harmonizing the crediting horizon also moves our ERW estimates closer to published ranges, although those ranges rest on different accounting conventions. At $H = 25$ our values fall to \$110–\$178/tCO_2 for basalt and \$28–\$33/tCO_2 for dunite, below the \$200 and \$60/tCO_2 reported for the two rocks by Strefler et al.[55]. A main difference is that a steady-state supply curve that credits the rock mass weathering each year at its full stoichiometric potential and that does not cover the CO_2 emitted during mining, grinding, and spreading. The basalt values also lie inside the \$50–\$200/tCO_2 range assessed by Fuss et al.[18], a synthesis of the earlier literature, and the \$80–\$180/tCO_2 removal costs reported for 2050 deployment by Beerling et al.[96]. The remaining differences reflect input choices, mainly grain size, transport distance, and electricity price, together with our deduction of co-product revenue.

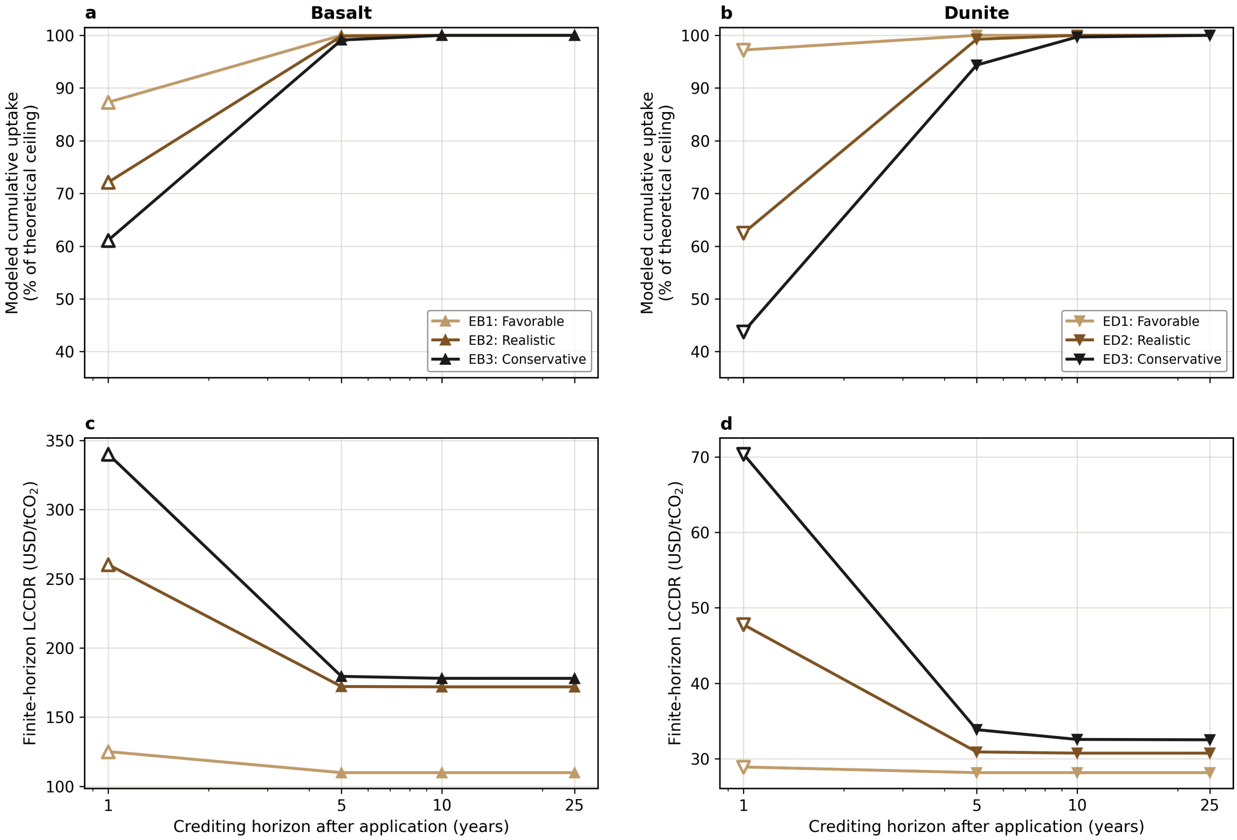

Supplementary Figure 9. ERW removal crediting. Panels **a** and **b** show modeled cumulative uptake relative to the stoichiometric ceiling for basalt and dunite. Panels **c** and **d** report the corresponding LCCDR after discounting each year's credited uptake. Open markers identify the main one-year convention; filled markers extend the crediting horizon to 5, 10, and 25 years. Curves that visually meet the ceiling do so only at plotting precision; the calculation retains a positive residual and does not assume complete physical uptake.